IMBIBITION ASSISTED OIL RECOVERY

A Thesis

by

ORKHAN H. PASHAYEV

Submitted to the Office of Graduate Studies of
Texas A&M University
in partial fulfillment of the requirements for the degree of

MASTER OF SCIENCE

August 2004

Major Subject: Petroleum Engineering

IMBIBITION ASSISTED OIL RECOVERY

A Thesis

by

ORKHAN H. PASHAYEV

Submitted to Texas A&M University
in partial fulfillment of the requirements
for the degree of

MASTER OF SCIENCE

Approved as to style and content by:

_____   _____
David S. Schechter   J. Bryan Maggard
(Chair of Committee)   (Member)

_____   _____
Wayne M. Ahr   Stephen Holditch
(Member)   (Head of Department)

August 2004

Major Subject: Petroleum Engineering

ABSTRACT

Imbibition Assisted Oil Recovery. (August 2004)

Orkhan H. Pashayev, B.S., Azerbaijan State Oil Academy

Chair of Advisory Committee: Dr. David S. Schechter

Imbibition describes the rate of mass transfer between the rock and the fractures. Therefore, understanding the imbibition process and the key parameters that control the imbibition process is crucial. Capillary imbibition experiments usually take a long time, especially when we need to vary some parameters to investigate their effects. Therefore, this research presented the numerical studies with the matrix block surrounded by the wetting phase for better understanding the characteristic of spontaneous imbibition, and also evaluated dimensionless time for validating the scheme of upscaling laboratory imbibition experiments to field dimensions.

Numerous parametric studies have been performed within the scope of this research. The results were analyzed in detail to investigate oil recovery during spontaneous imbibition with different types of boundary conditions. The results of these studies have been upscaled to the field dimensions. The validity of the new definition of characteristic length used in the modified scaling group has been evaluated. The new scaling group used to correlate simulation results has been compared to the early upscaling technique.

The research revealed the individual effects of various parameters on imbibition oil recovery. Also, the study showed that the characteristic length and the new scaling technique significantly improved upscaling correlations.

DEDICATION

This thesis is dedicated to my daughter Emilia.

ACKNOWLEDGEMENTS

TABLE OF CONTENTS

LIST OF FIGURES

FIGURE   Page

LIST OF TABLES

CHAPTER I

INTRODUCTION

1.1 Naturally Fractured Reservoirs

It has been estimated that 30% of the oil production of the world comes from naturally fractured reservoirs. Naturally fractured reservoirs are typically considered as a dual-porosity system, which is composed of two distinct media: the matrix and the fractures. The matrix has high porosity but low permeability, and the fractures have very high permeability and low porosity. This combination means that most of oil and gas is stored in the matrix and the fractures system provides the main channel for fluid flow. A successful recovery process is the one that recovers hydrocarbon from the low-permeability high-porosity matrix. Because of the interactions between the matrix and the fracture, the characteristics of the fluid flow in the naturally fractured reservoirs are quite different from those of conventional single-porosity reservoirs. Some of the tasks in the recent modeling studies of naturally fractured reservoirs include the following main steps: geological fracture characterization, hydraulic characterization of fractures, upscaling of fractured reservoir properties, and fractured reservoir simulation.

During the past decades, the modeling of naturally fractured reservoirs has advanced considerably because of the desire to increase recovery from naturally fractured formations and to exploit the vast storage capacity of naturally fractured oil reservoirs for the underground disposal of nuclear wastes. There are two common modeling methods of naturally fractured reservoirs:

_____

This thesis follows the style of the *SPE Reservoir Evaluation & Engineering Journal.*

- Numerical models with sufficiently refined grids to adequately represent matrix/fracture geometry.
- Dual porosity models which assume fractures and rock matrix as two superimposed continuous porous media.

In the dual porosity model, the fluid flow between the matrix blocks and the surrounding fractures is characterized by the transfer functions. For the transfer functions, it is a prerequisite that they accurately describe the multiphase flow between the matrix and the surrounding fractures. The expulsion of oil from the matrix blocks to the surrounding fractures by capillary imbibition of water is one of the most important oil recovery mechanisms in naturally fractured reservoirs with the low-permeability rock matrix, since in such reservoirs the conventional methods of production, such as building a pressure difference across matrix blocks, fail because of the high-permeability fracture network.

1.2 Capillary Imbibition

Capillary imbibition is described as a spontaneous penetration of a wetting phase into a porous media while displacing a non-wetting phase by means of capillary pressure, e.g., water imbibing into an oil-saturated rock. Imbibition plays an important role in the recovery of oil from naturally fractured reservoirs. The schematic representation of the imbibition process is presented in **Fig 1.1.**
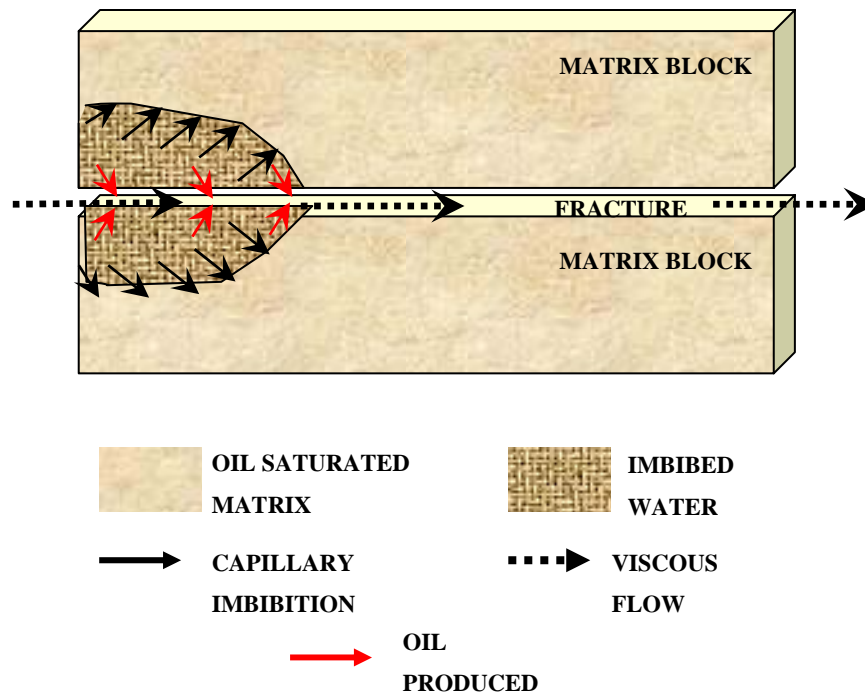
Fig 1.1—Schematic representation of the displacement process in fractured media

Imbibition describes the rate of mass transfer between the rock and the fractures. Therefore, understanding the imbibition process and the key parameters that control the imbibition process is crucial.

Imbibition occurs when the porous solid containing a fluid comes into contact with another fluid that more preferably wets the solid. If the porous solid is an oil containing reservoir with oil saturation above the residual value, then water imbibing into the pore space may displace a portion of this trapped oil out of the matrix through a replacement mechanism. This imbibition mechanism may be employed to produce oil from the porous reservoirs formed by the invasion of oil into the pore matrix over geological time periods. Normally, these porous oil reservoirs contain both oil and water (called connate water). If this type of reservoir

is water wet, the trapped oil is a candidate for recovery by the imbibition water soak process. Oil recovery by this imbibition process is accomplished by contacting water with the porous solid. The water is then imbibed into the pore matrix, where upon reaching regions of oil saturation, the water will encroach along the solid surface causing a portion of trapped oil to be displaced. In the typical fractured low- permeability reservoirs, most of the trapped oil is contained in the pore matrix itself with remaining oil residing in the fractures. Primary oil production accounts mainly for oil recovery from these fractures and the rock matrix very near the fractures. Attempts to recover the substantial amount of trapped oil in the matrix by the secondary production processes are generally inefficient, because injected fluid tends to channel through the fracture network to the production site, bypassing large amounts of oil trapped in the pore matrix.

Water imbibition is an alternative enhanced oil production strategy capable of recovering a portion of this trapped oil through a replacement mechanism that exchanges water for oil. The effectiveness of this process depends on several parameters, including matrix block size, rock porosity and permeability, fluid viscosities, interfacial tensions, and rock wettability. The process is also a function of the contact area between the imbibing fluid and the rock matrix. For this reason, fractured porous oil reservoirs are the best candidates for oil recovery by the water soak imbibition process because the natural fractures provide an extremely large fluid to rock contact area. In this manner, the reservoir may be visualized as a combination of many small oil production blocks separated by the fracture zones rather than a single large oil production block.

Water imbibition is a primary component of fluid transfer from the matrix to the fracture. Two approaches are generally used to describe the flow from the matrix blocks to the fractures and within the matrix blocks themselves: numerical and analytical. Numerical modeling requires intensive computer programming. The

relations among the model parameters are often obscured inside of complex non-linear expressions. Analytical solutions may provide more necessary physical insights about the effect of the model parameters and help better understand imbibition mechanisms to predict and optimize oil recovery. In turn, this can help to refine existing numerical models and/or develop better models in the future.

1.3 Research Problem

Different critical aspects of the capillary imbibition process have received a limited treatment in the petroleum literature. None of the recent papers devoted to capillary imbibition studies investigated the numerical scale-up of the process. Most authors checked the validity of their numerical models against data from the imbibition tests involving the same boundary conditions. Early scaling studies of spontaneous imbibition mostly focused on the shape factor, while there is no emphasis on end-point mobilities. Large discrepancies among the scaled curves brought up the effect of sample heterogeneity, which is not well studied yet.

1.4 Objectives

The objectives of the present study are to conduct numerical studies with the matrix block surrounded by the wetting phase for better understanding the characteristic of spontaneous imbibition, and also evaluate dimensionless time for validating the scheme of upscaling laboratory imbibition experiments to field dimensions. The purpose here is to isolate the individual effects of various parameters on imbibition recovery. This study addresses the importance of characterizing the imbibition mechanism for analysis of reservoir performance.

1.5 Methodology

Capillary imbibition experiments usually take a long time, especially when we need to vary some parameters to investigate their effects. Therefore, to achieve the objectives of the present study, numerical modeling of the spontaneous imbibition experiment was performed using a two-phase black-oil commercial simulator (CMG™). The experimental results from water static imbibition experiments performed by Yan Fidra[1] have been acquired.

Numerous parametric studies were performed and the results were analyzed in detail to investigate oil recovery during spontaneous imbibition with different types of boundary conditions. These studies included the effect of varying mobility ratio, different fracture spacing, different capillary pressure, different relative permeabilities, and varying permeability profiles along the core.

The results of these studies were upscaled to the field dimensions. The validity of the new definition of characteristic length used in the modified scaling group was evaluated based on our model. The new scaling group used to correlate simulation results was compared to early upscaling technique.

1.6 Outline of Thesis

In this report the study has been divided into chapters. Chapter II presents a detailed literature review on various aspects of spontaneous imbibition and also pertinent information on the upscaling of experimental results from a spontaneous imbibition process.

Chapter III describes the spontaneous imbibition experiments conducted by Yan Fidra and data available from his experimental work. Experimental procedures,

including core treatment and followed by spontaneous imbibition tests, are explained in detail. Chapter IV describes numerical modeling of spontaneous imbibition experiments using a two-phase black-oil commercial simulator (CMG^{TM}). This chapter includes grid sensitivity analysis, matching laboratory experiment with numerical model, parametric studies, and detailed analysis of the results to investigate oil recovery during spontaneous imbibition. Chapter V presents the upscaling of static imbibition results to the field dimensions. The final chapter concludes the thesis.

CHAPTER II

BACKGROUND AND LITERATURE REVIEW

This chapter presents a detailed literature review on various aspects of spontaneous imbibition and also pertinent information on the upscaling of experimental results from spontaneous imbibition process.

2.1 Fluid Flow Modeling in Naturally Fractured Reservoirs

Fractures are defined as "naturally occurring macroscopic planar discontinuities in rock due to deformation or physical digenesis.[2]" Fractured reservoirs, according to Nelson[2] can be divided into four types, **Table 2.1**:

Table 2.1—Types of Fractured Reservoirs

Reservoir Type	Definition	Examples
Type 1	Fractures provide essential porosity and permeability.	Amal, *Libya* Ellenburger fields, *Texas* Edison, *California* PC Fields, *Kansas*
Type 2	Fractures provide essential permeability	Agha Jari, *Iran* Haft Kel, *Iran* Sooner Trend, *Oklahoma* Spraberry Trend Area, *Texas*
Type 3	Fractures provide a permeability assistance	Kirkuk, *Iraq* Dukhan, *Qatar* Cottonwood Creek, *Wyoming* Lacq, *France*
Type 4	Fractures provide no additional porosity or permeability, but create significant reservoir anisotropy.	Pineview, *Utah* Beaver Creek, *Alaska* Hugoton, *Kansas*

The porous system of any reservoir can usually be divided into two parts:

- Primary Porosity, which is usually intergranular and controlled by lithification and deposition processes.
- Secondary Porosity, which is caused by post-lithification processes, such as fracturing, jointing, solution, recrystalization and dolomitization.

The void systems of sands, sandstones, and oolitic limestones are typical for primary porosity. Typical for secondary porosity are vugs, joints, fissures, and fractures. Naturally fractured reservoirs form a challenge to the engineers and geologists due to their complexities. These reservoirs have millions of barrels of oil left unrecovered due to the poor knowledge of the reservoirs. Therefore, the studies of naturally fractured reservoirs have gained importance over the years. And the substantial research studies have been accomplished in the area of geomechanics, geology and reservoir engineering of fractured reservoirs.[3-8]

Warren and Root[9] first introduced the concept of dual porosity medium and presented an analytical solution for the single-phase, unsteady-state flow in a naturally fractured reservoir. Their idealized dual model is widely used in today's commercial reservoir simulators to simulate the fluid flow in naturally fractured reservoirs. In their model, the isolated cubes represent the matrix blocks and the gaps between cubes represent well-connected fractures, as shown in **Fig 2.1.** The fracture system is further assumed to be the primary flow paths, but it has negligible storage capacity. Also, the matrix is assumed to be the storage medium of the system with negligible flow capacity. The idealization made the following assumptions:

- The primary porosity is homogeneous and isotropic, and is contained within a systematic array of identical, rectangular parallelepipeds.

- All of the secondary porosity is contained within an orthogonal system of continuous, uniform fractures, which are oriented parallel to the principal axes of permeability.
- The flow can occur between the primary and secondary porosities, but the flow through the primary-porosity elements can not occur.
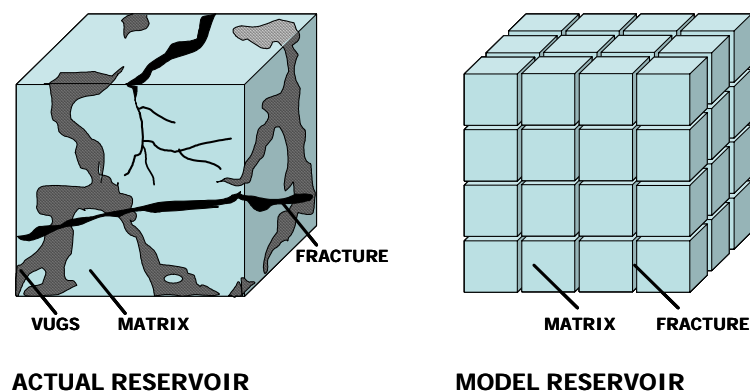
Fig 2.1—Idealization of dual porosity reservoir

The primary and secondary porosities are coupled by a factor called the transfer function or the inter-porosity flow. Physically, this can be defined as the rate of the fluid flow between the primary and secondary porosities. Since the secondary porosity is the only fluid path and it lacks in fluid storage, the dual porosity simulation method can be imagined as a system of the secondary porosity with the primary porosity as the only source of fluids. Transfer functions assume that the transfer or inter-porosity flow can be attributed to imbibition phenomenon.

2.2 Imbibition Flooding

The importance of capillary imbibition was identified by the early investigators. Brownscombe and Dyes suggested that imbibition flooding could contribute to oil production from the Spraberry trend of West Texas.[10] This study established that for applying successful imbibition flood, the rock has to be preferentially water-wet and the rock surface exposed to imbibition should be as large as possible. Kleppe and Morse[11] suggested a two-dimensional numerical model which was able to simulate flow of water and oil in the matrix block as well as in the fractures. The fractures were represented by horizontal and vertical flow channels surrounding the matrix blocks.

The published studies have been concerned with different conditions under which water imbibition occurs. Geometrical shape and size of the samples, boundary conditions, effects of gravity, type of fluids, and flowing conditions of the fluid surrounding the rock blocks are among the many factors that have been considered. Oil recovery by water imbibition displacement has concentrated on evaluating the relationship between time and oil production rate. **Fig. 2.2** shows a typical curve of time versus oil recovery by water imbibition.
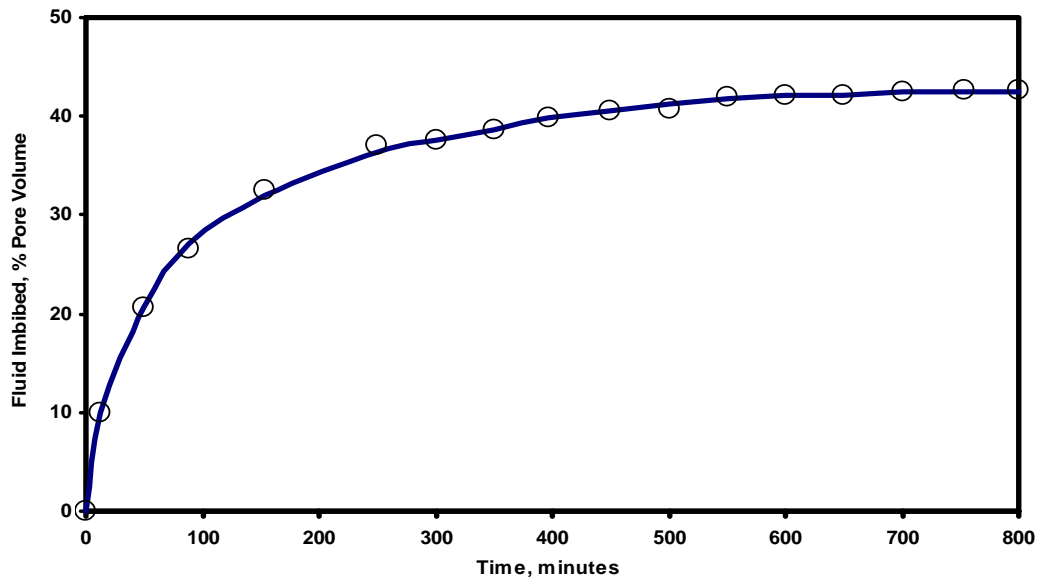
Fig 2.2—Typical production curve for imbibition[12]

In dealing with imbibition, it is vital to consider capillary pressure. Capillary pressure is a basic parameter that relates the pressures of the wetting and non-wetting fluid in the porous media. Generally capillary pressure is expressed as the pressure of a non-wetting phase minus the pressure of a wetting phase, and this relation known as the Laplace equation is given by,

$$P_c = P_{nw} - P_w = \frac{2\sigma}{r}\cos\theta, \quad \dots\dots\dots\dots\dots\dots\dots\dots \quad (2.1)$$

where σ is the interfacial tension between a wetting and a non-wetting phase, r is the pore radius, and θ is the contact angle measured through the wetting phase. Thus, capillary pressure is a strong function of pore size. The rocks with large pore size will exhibit lower capillary forces in contrast to the rocks with small pores that can generate larger capillary forces. A pore size and pore size distribution influence the capillary pressure curve shape.

Capillary pressure is not a unique function of saturation as it depends on the saturation history and the direction of saturation change.[13] A primary drainage curve is obtained when a porous medium begins from 100% water saturation and is subsequently drained to a minimum value, S_{wi} followed by the imbibition curve, when water saturation increases again from S_{wi} to a maximum value S_{nwr}, residual saturation. If the porous medium is drained again, a secondary drainage curve can be obtained.

In **Fig. 2.3** we observe that beyond the irreducible saturation S_{wi}, a wetting phase is no longer continuous, hence further pressure change does not result in additional desaturation. Similarly, an imbibition curve terminates at a maximum saturation S_{nwr}, which is lower than 100%, due to the amount of the non-wetting fluid which remains trapped in the form of isolated blobs. The remaining non-wetting fluid is called a non-wetting phase residual saturation.
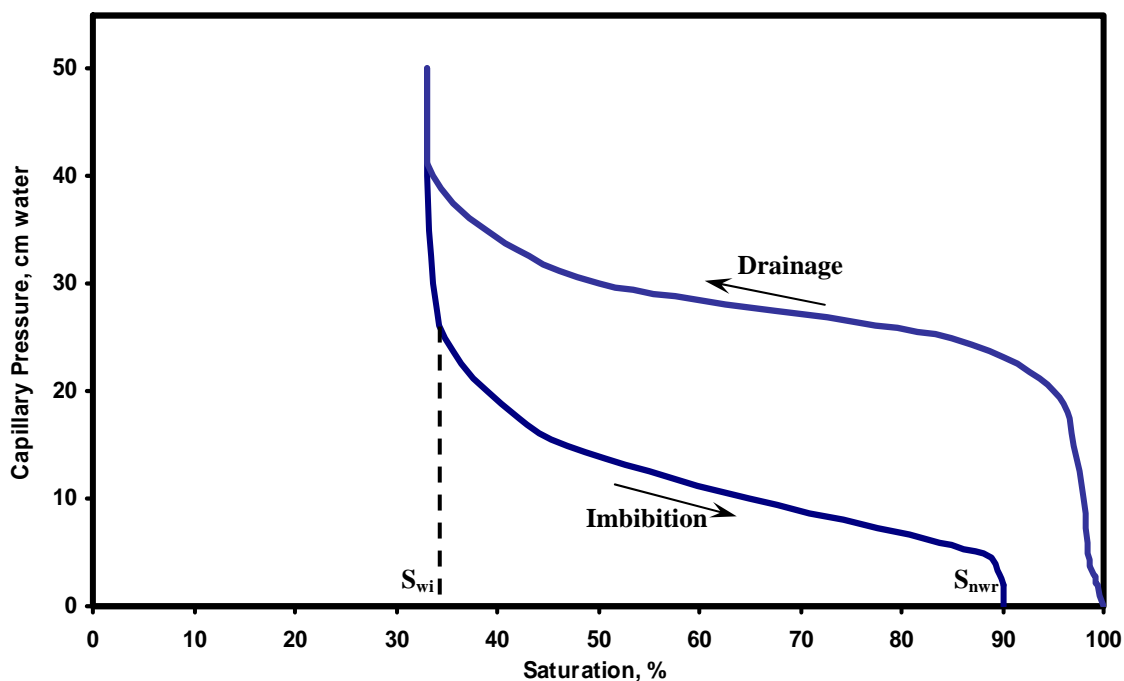
Fig 2.3—An example of Capillary Pressure Plot function[14]

Another characteristic value is the capillary pressure at the point of injection of a drainage path, which is called the displacement pressure or the entry pressure. This is the minimum pressure difference required for the non-wetting fluid to displace the wetting one and is also called the threshold capillary pressure. Before this value is reached, saturation remains constant, while the capillary pressure is increasing and only when it is exceeded, does the actual desaturation take place. Several empirical and semi-empirical expressions have been proposed to correlate the capillary pressure, medium properties, and fluid properties to phase saturation.

Brooks and Corey[15] arrived at one of such power expressions, which is given by,

$$S_e = \left(\frac{P_e}{P_c}\right)^{\lambda}, P_c > P_e, \quad \text{.. (2.2)}$$

where S_e is the effective water saturation, P_c is the capillary entry pressure, and λ is a fit parameter.

Leverett[16] came up with a function known as the Leverett J function, which is a unique function of saturation. For several different water-wet unconsolidated sands, he found a single characteristic curve. The Leverett J function is defined as:

$$J(S_w) = \frac{P_c}{\sigma \cos \theta} \sqrt{\frac{k}{\phi}}, \quad \text{.. (2.3)}$$

where k is the absolute permeability of the medium, ϕ is the porosity, and the ratio $(k/\phi)^{1/2}$ is interpreted as a characteristic mean pore or grain diameter.

2.3 Transfer Functions

As was mentioned earlier, the primary and secondary porosities are coupled by a factor called transfer function or the inter-porosity flow.[17] Transfer functions can be broadly classified to be of four types:

- Material Balance Transfer Functions.
- Diffusivity Transfer Functions.
- Empirical Transfer Functions.
- Scaling Transfer Functions.

Material Balance Transfer functions assume that the transfer of fluids from the matrix to the fracture can be adequately described by Darcy's Law with an appropriate geometric factor that accounts for the characteristic length and the flow area between the matrix and the fracture. Diffusivity Transfer functions assume that the inter-porosity flow can be approximated by "diffusion" phenomenon. These functions are based on incompressible flow and assume that the diffusivity equation[18] is sufficient to model the inter-porosity flow between the matrix and the fracture media. Empirical models assume the transfer or the inter-porosity flow can be attributed to imbibition phenomenon. They assume an exponential decline function to describe the time rate of exchange of oil and water for a single matrix block, when surrounded by the fractures with high water saturation.[19-26]

2.3.1 Scaling Transfer Functions

Scaling transfer functions are used to predict recovery in field size cases with the results from lab experiments. Rapoport[27] proposed the "scaling laws" applicable in case of oil/water flow. These laws are derived directly from Darcy's Law for the individual phases and the continuity equation. If the scaling conditions are met, the results from a laboratory will simulate the reservoir prototype behavior. Rapoport's

scaling laws require one type of relative permeability and similarly shaped capillary pressure curves for all porous media, but are still general enough to be applied to the imbibition process.

Using these laws, Graham and Richardson[28] developed a theoretical model for a system where capillary imbibition occurs only in one direction (1D). Their model considered linear imbibition, where a length of homogenous porous rock is assumed to be completely encapsulated, except for one surface designated the imbibition face. The term linear imbibition refers to the fact that the imbibing water advances only in one direction. If this rock is completely filled with oil and connate water, then imbibing water will flow in through the imbibition face displacing oil countercurrently out of the same imbibition face. This model used Darcy's Law, Leverett's reduced capillary pressure function, and the fact that the flow rate of water into the pore matrix, at any given point, is equal to the flow rate of oil in the opposite direction. The following equation was derived and formulated as the Graham/Richardson model for the flow of oil and water phases:

$$q_o(L,t) = -\sqrt{k\phi}A\sigma f(\theta)\left[\left(\frac{k_{rw}k_{ro}}{\mu_w k_{ro} + \mu_o k_{rw}}\right)\frac{dJ(S_w)}{d(S_w)}\frac{\partial S_w}{\partial L}\right]. \quad .. \quad (2.4)$$

Their conclusions were as follows:

- The rate of water imbibition varies with the square root of absolute permeability and interfacial tension between two liquids.
- The rate of water imbibition is a function of the viscosity of both oil and water.
- The rate of water imbibition is a complex function of relative permeability and capillary pressure.

Graham and Richardson implied that laboratory data could be scaled up to reservoir parameters to estimate oil recovery, which would probably eliminate the trouble of

finding precise values for many parameters in their model. In addition, Graham and Richardson concluded that the initial rate of imbibition and the amount of oil recovered were independent on the sample length and that at high flooding rates oil is produced due to large applied pressure gradients, while low injection rates produce oil through capillary pressure gradients, where imbibition is the dominant production mechanism. Furthermore, at higher injection rates more water had to be injected to produce a given amount of oil and the time required to produce that amount of oil did not decrease proportionally with injection rate. From these observations they concluded that for a given fracture width lower injection rates yielded better oil recoveries per amount of injected water.

Encouraged by Graham and Richardson's work, Mattax and Kyte[29] developed the following relationship, which can be used for scaling laboratory data to field conditions:

$$\left[t\sqrt{\frac{k}{\phi}} \frac{\sigma}{\mu_w L^2} \right]_{laboratory} = \left[t\sqrt{\frac{k}{\phi}} \frac{\sigma}{\mu_w L^2} \right]_{\substack{reservoir \\ matrix \\ block}} , \quad \text{.................} \quad (2.5)$$

where L is core length. However, to use Mattax and Kyte's scaling relation, the following restrictions have to be satisfied:

- Gravity effects are negligible.
- The shape of a laboratory model is identical to that of the reservoir matrix block.
- The laboratory model has the same oil/water viscosity ratio as that of the reservoir.
- The laboratory model duplicates the initial fluid distributions in the reservoir matrix block and the pattern of water movement in the surrounding fractures.

- Relative permeabilities as the functions of fluid saturation are the same for the reservoir matrix block and the laboratory model.
- The capillary pressure of the reservoir matrix block and the laboratory model are related by direct proportionality, such as Leverett's dimensionless J-function.

Mattax and Kyte performed 1D and 3D imbibition experiments to examine their scaling relations. They showed that the imbibition time could be normalized using a dimensionless time:

$$t_D = t \sqrt{\frac{k_m}{\phi}} \frac{\sigma}{\mu_W} \frac{1}{L^2} \ . \ \dots\dots\dots\dots\dots\dots\dots\dots\dots\dots\dots\dots \ (2.6)$$

Mattax and Kyte's scaling relation is not restricted to any dimensions and is applicable to any arbitrary shape matrix block, provided that the shape of the reservoir matrix block is duplicated in the laboratory model. It is a major difficulty to duplicate the relative permeability and capillary pressure functions of a reservoir matrix block in laboratory systems. Mattax and Kyte, however, claimed that these functions would be automatically matched if rock samples from the reservoir itself were used. The one unique advantage of Mattax and Kyte's scaling relation is that it can be used for both co-current and countercurrent imbibition, since it does not put a restriction on the direction of flow.

Blair[30] presented an analytical solution of the equations describing the effects of water imbibition and oil displacement. The water imbibition studies were conducted on both linear and radial systems. Changes in capillary pressure and relative permeability curves, initial water saturation, and oil viscosity were observed as a result of variation of imbibition rates. These parameters were evaluated as the functions of time. The time required to imbibe a fixed amount of water was approximately equal to the square root of the reservoir oil viscosity if oil viscosity was greater than water viscosity.

Du Prey[31] performed imbibition experiments on cores within centrifuges to account for gravity effect on imbibition. In his work, he showed discrepancy among the scaled recovery curves corresponding to different block sizes. Du Prey defined three more dimensionless parameters:

- Dimensionless Shape factor.
- Dimensionless mobility.
- Capillary to gravity ratio.

The dimensionless time was defined for two cases: low capillary to gravity ratio and for high capillary to gravity ratio

$$t_c = \frac{H^2 \phi \Delta S \mu_o}{P_{ct} k_{o\,max}}, \quad \text{..} \quad (2.7)$$

$$t_g = \frac{H \phi \Delta S \mu_o}{\Delta \rho g k_{o\,max}}, \quad \text{..} \quad (2.8)$$

where t_c is dimensionless time factor for high capillary gravity ratio and t_g is dimensionless time factor for low capillary gravity ratio. Du Prey's model can be applied to any arbitrary shaped matrix block. However, experimental studies by Du Prey did not verify the above scaling parameters.

Hamon and Vidal[32] performed a set of laboratory imbibition tests. They showed that use of conventional scaling laws could sometimes lead to errors in recovery rate predictions because of heterogeneity of rock samples.

Bourblaux and Kalaidjian[33] studied co-current and countercurrent imbibition. They came up with the conclusion that the effects of heterogeneities of the porous medium on the spatial distribution of the fluids should be taken into account in

modeling to separate the effects of viscous coupling from those of macroscopic heterogeneities.

Kazemi *et al.*[34] presented an improved version of Mattax and Kyte's scaling relation in terms of the matrix block shape factor:

$$t_D = \left[\sqrt{\frac{k}{\phi} \left(\frac{\sigma F}{\mu} \right)} \right] t \ , \ \dots\dots\dots\dots\dots\dots\dots\dots \ (2.9)$$

where the shape factor, F_s is defined as

$$F = \frac{1}{V_{ma}} \sum \frac{A_{ma}}{d_{ma}} \ , \ \dots\dots\dots\dots\dots\dots\dots\dots \ (2.10)$$

and V_{ma} is the volume of the matrix block, A_{ma} is the area of a surface open to flow in a given direction, and d_{ma} is defined by the shape and boundary conditions of the matrix block.

Akin, Kovsek and Schembre[35] and later Akin and Kovsek[36] observed that both water/air and oil/water imbibition results in diatomite can be correlated with a single dimensionless function. Moreover, they noticed that imbibition fronts in the absence of initial water saturation are sharp, suggesting that during spontaneous imbibition pores of all sizes fill simultaneously.

Ma *et al.*[37] studied the relationship between water wetness and oil recovery from imbibition. They modified the dimensionless scaling parameter of Mattax and Kyte. In their work, authors showed that for water/oil systems the imbibition rate is proportional to the geometric mean of the water and oil viscosities:

$$\mu_g = \sqrt{\mu_w \mu_o} \ . \ \dots\dots\dots\dots\dots\dots\dots\dots \ (2.11)$$

Also Ma *et al.* introduced the idea of characteristic length into dimensionless scaling parameter. A characteristic length can be defined for the systems with different boundary conditions:

$$Lc = \sqrt{\frac{V_b}{\sum_{i=1}^{n} \frac{A_i}{l_{A_i}}}} \,, \quad \text{... (2.12)}$$

where l_{Ai} is the length defined by the shape and boundary conditions of the matrix block, V_b is bulk volume of the matrix, and A_i is the area open to imbibition at the ith direction. So, depending on all these factors, Ma *et al.* came up with the different formulations for characteristic lengths.

CHAPTER III

DESCRIPTION OF SPONTANEOUS IMBIBITION EXPERIMENT

AND DATA ACQUISITION

This chapter describes the spontaneous imbibition experiments conducted by Yan Fidra and data available from his experimental work. The experimental procedures, including core treatment and followed by spontaneous imbibition tests, are explained in detail.

3.1 Materials

The material used in the experimental work consisted of Berea outcrop and synthetic brine. Berea sandstone was selected because it is widely used as a standard porous rock for experimental work in the petroleum industry.

Before being used, the core sample was dried at an ambient temperature. Then the sample was dried in an oven at 110 °C for at least 3 days and cooled in a vacuum chamber.

3.2 Experimental Procedures

First, the cleaning process was performed. The objective of core cleaning was to remove all organic compounds without altering the basic pore structure of the rock. To clean very tight core sample traditional toluene Dean-Stark extraction, which removes water and light components by boiling, was used. To insure the core sample was really clean, the process was then followed by injecting chloroform into the core sample. Then clean core was dried in an oven at 110 °C for 3 days.

3.2.1 Saturating the Core with Brine

Dry core sample was weighted on a balance after measurement of air permeability. The core sample was then saturated with deaerated brine using a vacuum pump for at least 12 hours. After saturating the core sample with brine, a period of about 3 days was allowed for the brine to achieve ionic equilibrium with the rock. The porosity and pore volume of the core were determined from the dry and saturated weights of core sample, bulk volume, and brine density. Then the core sample was inserted into a Hassler core holder using a confining pressure of 500 psig to measure the core absolute permeability to brine.

3.2.2 Establishing Initial Water Saturation

The core sample was saturated with oil by injecting oil through the core confined in a Hassler core holder with a confining pressure of 500 psig to establish initial water saturation.

The oil flooding pressure applied varied from a few psi to 50 psig with oil throughput ranging from 2 to 10 pore volumes, depending on the initial water saturation desired. In establishing initial water saturation, the direction of flooding was reversed halfway through the oilflooding cycle to minimize unevenness in saturation distribution. The lowest initial water saturation achieved was 30%.

For lower initial water saturations, high viscosity paraffin oil was injected into the core sample, until initial water saturation was achieved. Then about 10 pore volumes of oil were injected into the core to displace paraffin oil. The initial water saturation achieved using this method was about 25%.

3.2.3 Spontaneous Imbibition Test

The spontaneous imbibition tests were performed using an imbibition apparatus shown in **Fig. 3.1.** As can be seen from the figure, the apparatus is a simple glass container equipped with a graduated glass cap. To perform an imbibition test, a core sample was immersed in the glass container filled with preheated brine. The container was then covered with a graduated cap. After filling the cap full with brine, the container was then stored in an air bath that had been set at constant temperature of 138 °F. Due to capillary imbibition action, oil was displaced from the core sample by the imbibing brine. The displaced oil accumulated in the graduated cap by gravity segregation. During the experiment, the volume of produced oil was recorded against time. Before taking the oil volume reading, the glass container was gently shaken to expel oil drops adhered to the core surface and the lower part of the cap, so that all of the produced oil accumulated in the graduated portion of the glass cap. At the early stage of the test, the oil volume was recorded every ½ hour, while near the end of the test the oil volume was recorded every 24 hours. Excluding the core preparation, the test was completed within 21 days.

Air Bath

Oil recovered

Oil bubble

Glass funnel
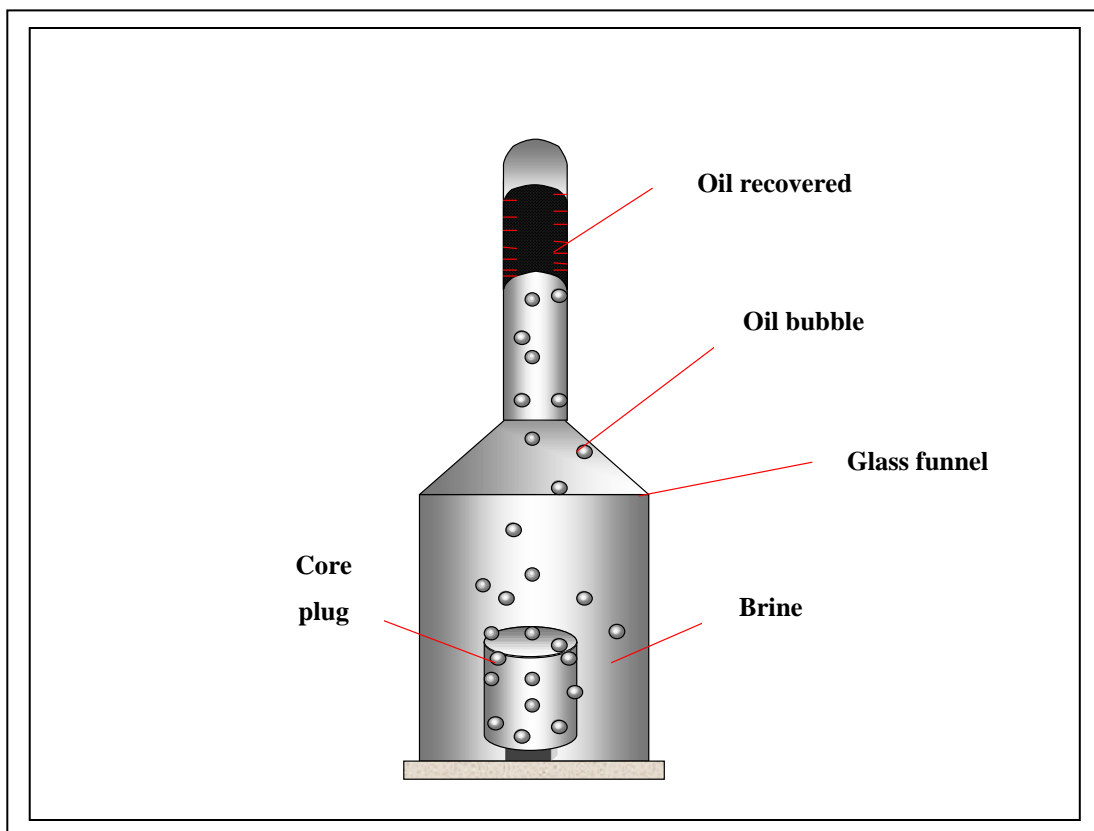
Core
plug

Brine

Fig. 3.1—Spontaneous imbibition cell

3.3 Data Available

The physical properties of the core sample and synthetic brine are listed in **Table 3.1.**

Table 3.1—Physical Properties of the Core and Brine

Property	Value	Unit
Dimensions of the core	3.2 x 3.2 x 4.9	cm
Porosity	15.91	%
Permeability	74.7	md
Initial water saturation	41.61	%
Viscosity of oil	3.52	cp
Density of oil	0.8635	g/cm^3
API	31	°
Viscosity of water	0.68	cp
Density of water	1	g/cm^3

Table 3.2 shows the results of the spontaneous imbibition experiment performed in the lab and **Fig. 3.2** presents the cumulative oil production from the core sample as a function of time. The portion of the oil recovery curve corresponding to the early times represents maximum rate of imbibition and the deviation of the oil recovery curve is caused by slowing down the imbibition rate. The imbibition rate slows

down, as all the major channels of flow are already filled. Later, the curve completely bends over and the rate of imbibition is drastically reduced. At this stage, a very slow change in water saturation within time is observed in the core. The final water saturation in the core reached 55.32%.

Table 3.2—Oil Recovery from Static Imbibition Experiment

Time, hours	Volume of oil, cm3	Recovery, %IOIP
0	0	0
0.02	0.1	2.13
0.03	0.3	6.38
0.07	0.7	14.89
0.27	1.3	27.66
0.49	1.5	31.91
1.19	1.65	35.11
1.65	1.7	36.17
2.5	1.8	38.3
4.17	1.85	39.36
8.69	1.9	40.43
12.62	1.95	41.49
15.75	2	42.55
20.75	2	42.55
63.75	2.05	43.62
255.75	2.1	44.68
500	2.1	44.68
750	2.1	44.68

28
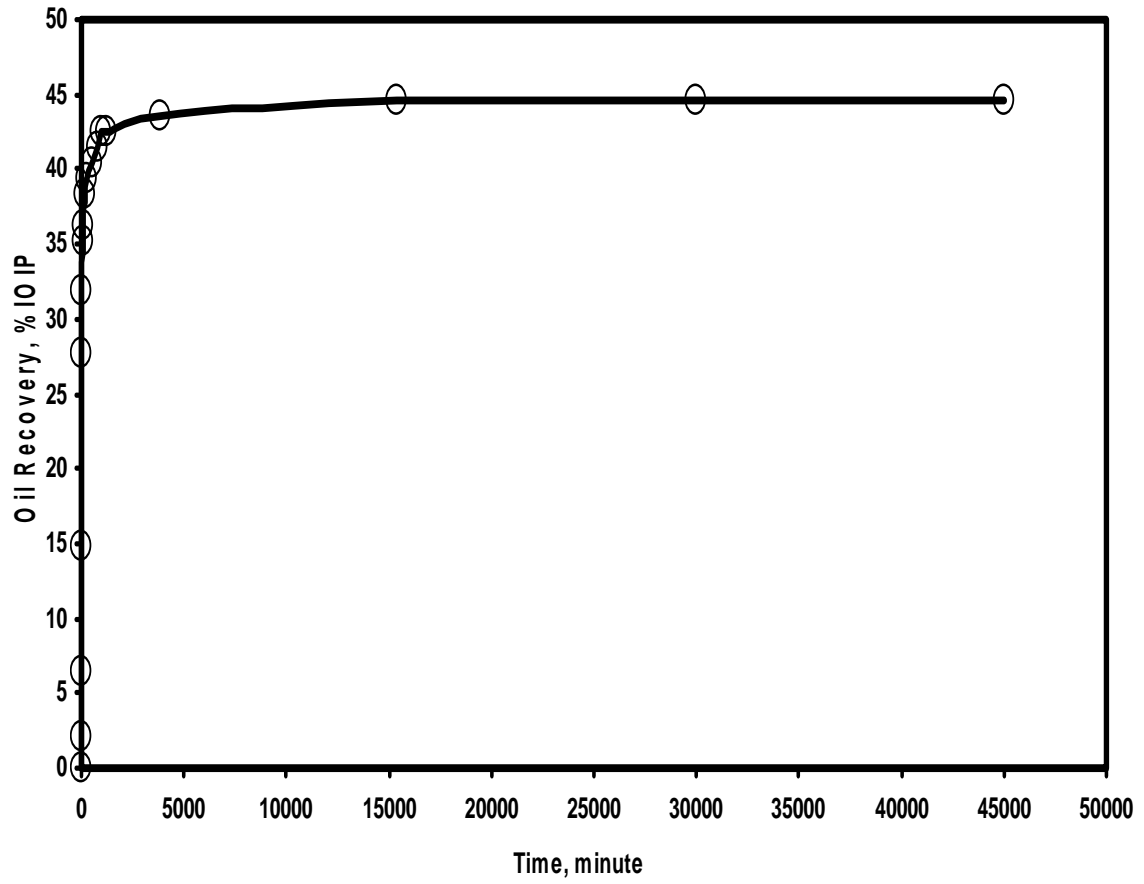
Fig 3.2—Oil recovery curve from static imbibition experiment

CHAPTER IV

NUMERICAL MODELING AND PARAMETRIC STUDIES OF

SPONTANEOUS IMBIBITION MECHANISM

This chapter describes a numerical modeling of spontaneous imbibition experiment using a two-phase black-oil commercial simulator (CMG^{TM}). The scope of this chapter includes

- Grid sensitivity analyses to determine an optimal grid size of the model.
- Matching laboratory cumulative oil production with a numerical model, to improve the agreement between model results and observed behavior from a laboratory experiment.[38-43] Investigation of oil recoveries of the numerical model with different types of boundary conditions. These boundary conditions are as follows:

  ➢ One End Open.
  ➢ Two Ends Closed.
  ➢ Two Ends Open.
  ➢ All Faces Open.

- Numerous parametric studies and detailed analysis of the results to investigate oil recovery during the spontaneous imbibition with different types of boundary conditions. These studies include the effect of varying mobility ratio, different fracture spacing, different capillary pressure, different relative permeabilities, and varying permeability profiles along the core.

4.1 Discretization of the Experiment and Grid Sensitivity Analysis

The core was completely surrounded by a wetting phase. Therefore, all faces of the core were at a constant water saturation of 1.0. All the rest of the core, prior to the experiment, was at constant initial water saturation, as was expressed by the initial conditions. Hence, the boundary conditions for this experiment were:

$$
\begin{aligned}
S_w(x, y, z, t) &= 1, x = 0 \\
S_w(x, y, z, t) &= 1, y = 0 \\
S_w(x, y, z, t) &= 1, z = 0 \\
S_w(x, y, z, t) &= 1, x = L_x \\
S_w(x, y, z, t) &= 1, y = L_y \\
S_w(x, y, z, t) &= 1, z = L_z
\end{aligned}
\qquad \ldots\ldots\ldots\ldots\ldots\ldots\ldots\ldots\ldots\ldots\ldots\ldots \quad (4.1)
$$

To simulate the experiment numerically, the core was discretized into a grid model. An extra gridblock of very small dimensions was added at the top, bottom, and all over the sides of the core to account for the boundary condition. This gridblock was assigned a water saturation value of 1.0. To keep this value constant at all times, the pore volume of this gridblock was multiplied by a huge number.

Grid sensitivity analysis has been performed to determine an optimal grid size of the model, to accurately represent fluid flow and yet maintain relatively fast simulation run. To investigate the sensitivity to a grid size, the initial model has been refined from coarse into fine grid. **Table 4.1** shows five grid sizes, which has been investigated in sensitivity analysis. The Cartesian grid system has been used.

Table 4.1—Table of Grid Sizes Investigated in the Grid Sensitivity Analyses

Number of Simulation Runs	Number of gridblocks in I, J, and K directions			Total number of gridblocks
	I-Direction	J-Direction	K-Direction	
1	7	7	7	343
2	12	12	12	1,728
3	16	16	16	4,096
4	20	20	20	8,000
5	20	20	25	10,000

Decision on an optimal grid size has been made based on the analysis of oil recovery curves and computer CPU times. The comparisons of results are shown in **Figs. 4.1** and **4.2.** Fig. 4.1 represents oil recovery curves vs. time for five grid sizes. From the figure it can be seen that although oil recoveries for the grid sizes $7 \times 7 \times 7$ and $16 \times 16 \times 16$ are different, as we refine the grid size the difference becomes very little. So, the difference in oil recoveries between the case with $20 \times 20 \times 20$ grid size and the case with $20 \times 20 \times 25$ grid size is almost negligible.
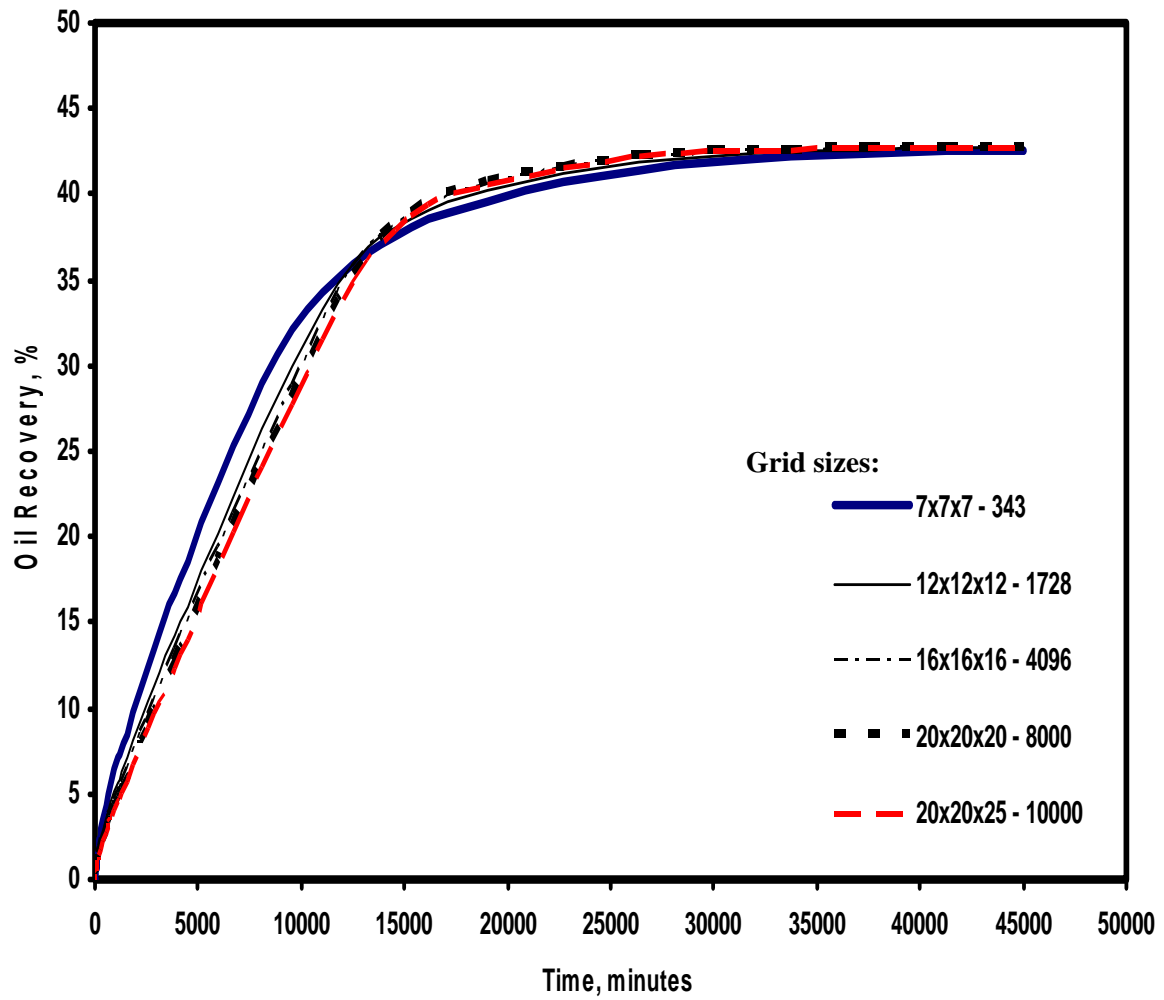
Fig. 4.1—Grid size effect on oil recovery from static imbibition experiment
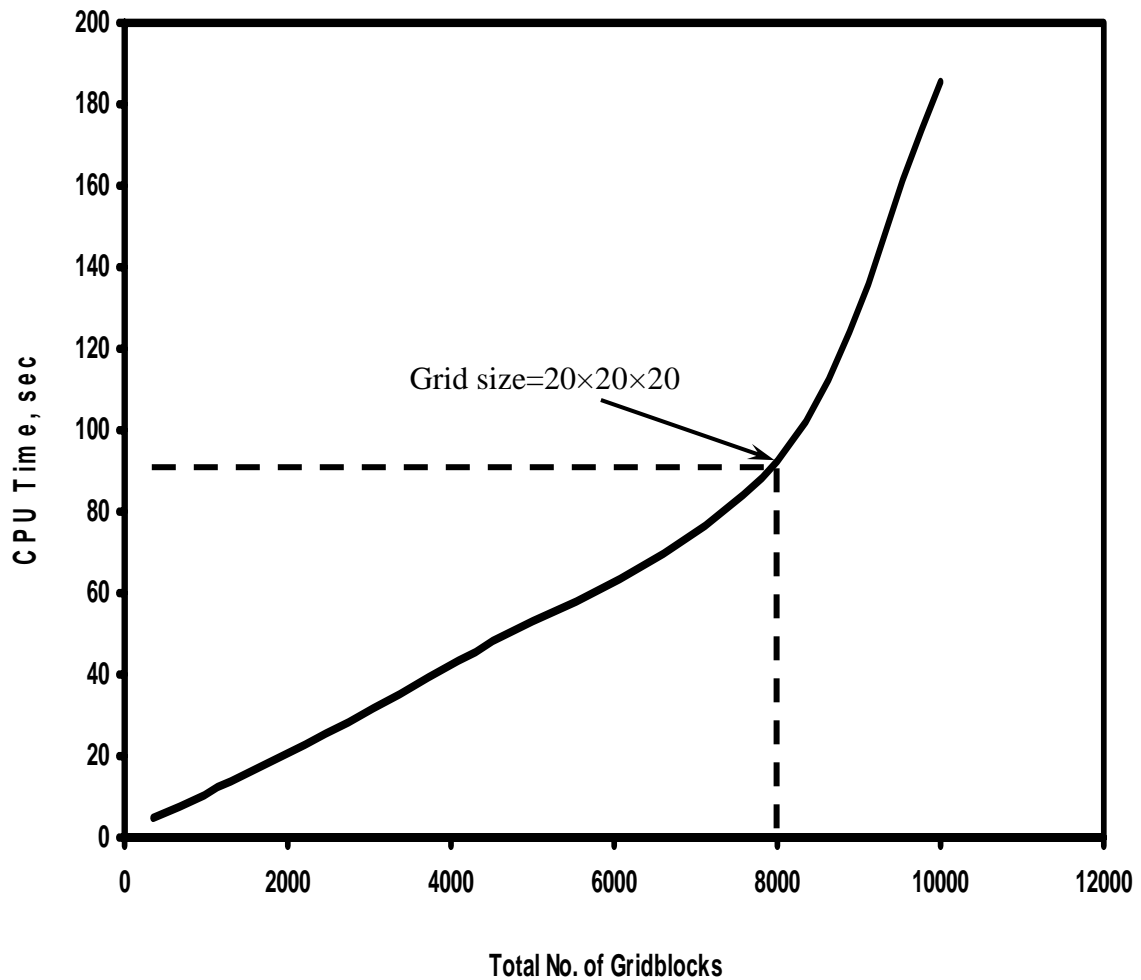
Fig. 4.2—Simulation times for different grid sizes

Fig. 4.2 has been developed to demonstrate the effect of the grid size refinement on the total simulation time, and also to help us determine the optimal number of gridblocks. According to the theory, the time for solving the pressure equation in

gridblock simulation increases exponentially. At a certain number of gridblocks, the exponential increase becomes more obvious. Our own analysis determined that this point occurred at 8,000 gridblocks, which corresponds to the grid size of 20×20×20.

So, based on the grid sensitivity analysis, the decision was made to use the grid size of 20×20×20. As can be seen from Fig. 4.2, it took around 90 seconds to simulate this case. Properties of the core after the grid sensitivity analysis for the further numerical simulation are represented in **Table 4.2.**

4.2 Matching Experimental Results

The primary objectives of matching were to improve and to validate the reservoir simulation data. In general, the use of the initial simulation input data does not match the historical reservoir performance to a level that is acceptable for making an accurate future forecast. The final matched model is not unique. In other words, several different matched models may provide equally acceptable matches to past reservoir performance, but may yield significantly different future predictions.

Table 4.2—Properties of the Core for Numerical Simulation

Property	Value	Units
Number of grid blocks in X-Direction	20	-
Number of grid blocks in Y-Direction	20	-
Number of grid blocks in Z-Direction	20	-
Grid Block Dimension X-Direction	0.178	cm
Grid Block Dimension Y-Direction	0.178	cm
Grid Block Dimension Z-Direction	0.242	cm
Density of oil	0.8635	g/cm^3
Density of water	1	g/cm^3
Viscosity of oil	3.52	cp
Viscosity of water	0.68	cp
Permeability	74.7	Md
Porosity	0. 1591	-
Initial Water Saturation	(2-19×2-19×2-19)*0.4161	-
Boundary Condition	All Sides	-

There is no way to avoid this problem, but matching as much production data as available and adjusting only the least known reservoir data within the acceptable ranges should yield a better match.[44]

In our own case, the only available data we had was the cumulative oil production from the core sample as a function of time (Table 3.2). This data was matched by trial and error estimates of relative permeability and capillary pressure. **Fig. 4.3** is a comparison of the observed oil recovery vs. simulated oil recovery. A very poor match could be observed from this figure.

4.2.1 Relative Permeability and Capillary Pressure

Relative permeability was modeled using the power law correlations built in the commercial simulator CMG™. The values of end-point permeabilities were varied to obtain the best match. The capillary pressure was modeled by trial and error solution.

Table 4.3 shows the relative permeabilities and the capillary pressure values obtained for this match. **Fig. 4.4** demonstrates the capillary pressure curve obtained for the model. The match of the recovery is shown in **Fig. 4.5.**
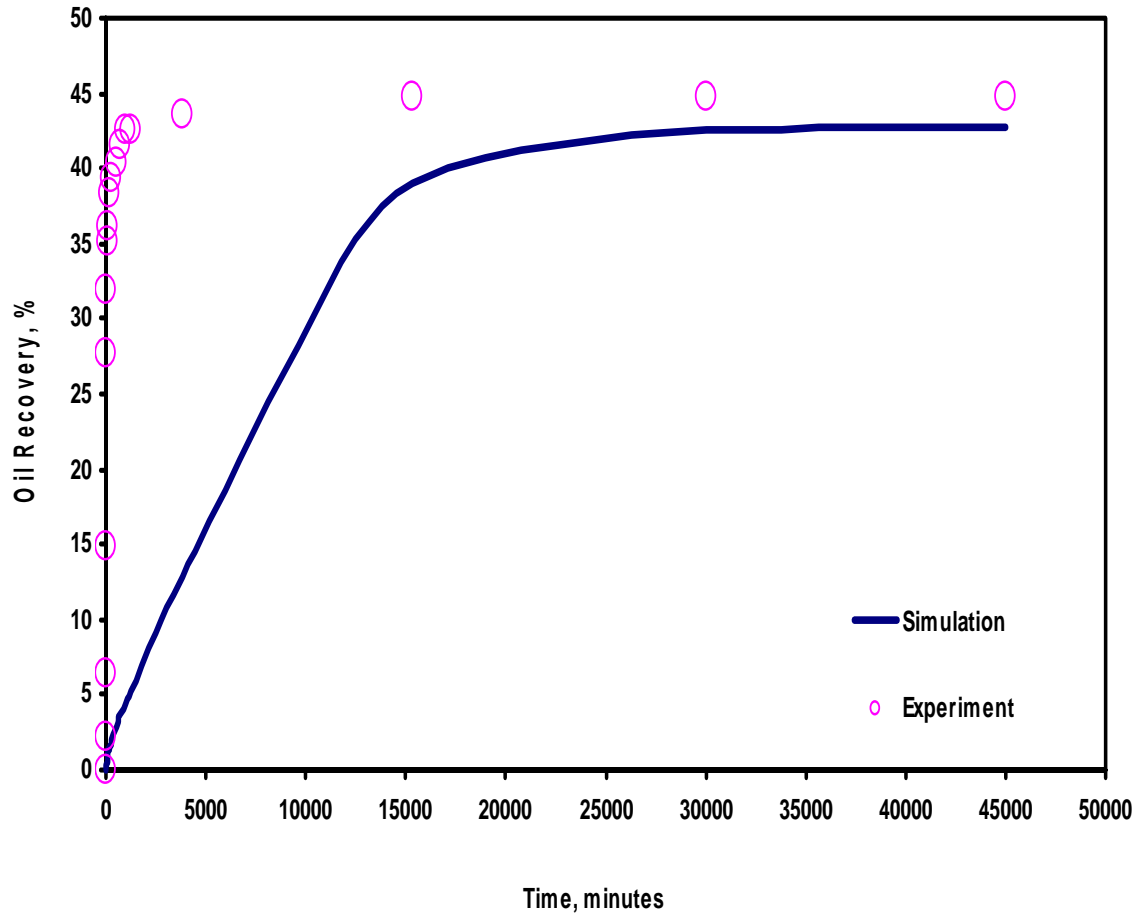
Fig. 4.3—Observed oil recovery vs. simulated before adjustment of reservoir data

Table 4.3—Table of Relative Permeabilities and Capillary Pressure

Water Saturation, Fraction	Water Relative Permeability	Oil Relative Permeability	Capillary Pressure, psi
0.4161	0	0.9	1.7537
0.4338	0.0007	0.7787	1.555
0.4516	0.003	0.6331	1.445
0.4693	0.0067	0.5069	1.373
0.4871	0.0119	0.3987	1.273
0.5048	0.0186	0.3071	1.164
0.5226	0.0268	0.2307	1.078
0.5403	0.0365	0.1682	0.976
0.5581	0.0476	0.1181	0.922
0.5758	0.0603	0.0791	0.828
0.5935	0.0744	0.0498	0.733
0.6113	0.09	0.0288	0.651
0.6290	0.1071	0.0148	0.547
0.6468	0.1257	0.0062	0.345
0.6645	0.1458	0.00018	0.254
0.6823	0.1674	0.00015	0.134
0.7	0.2	0	0
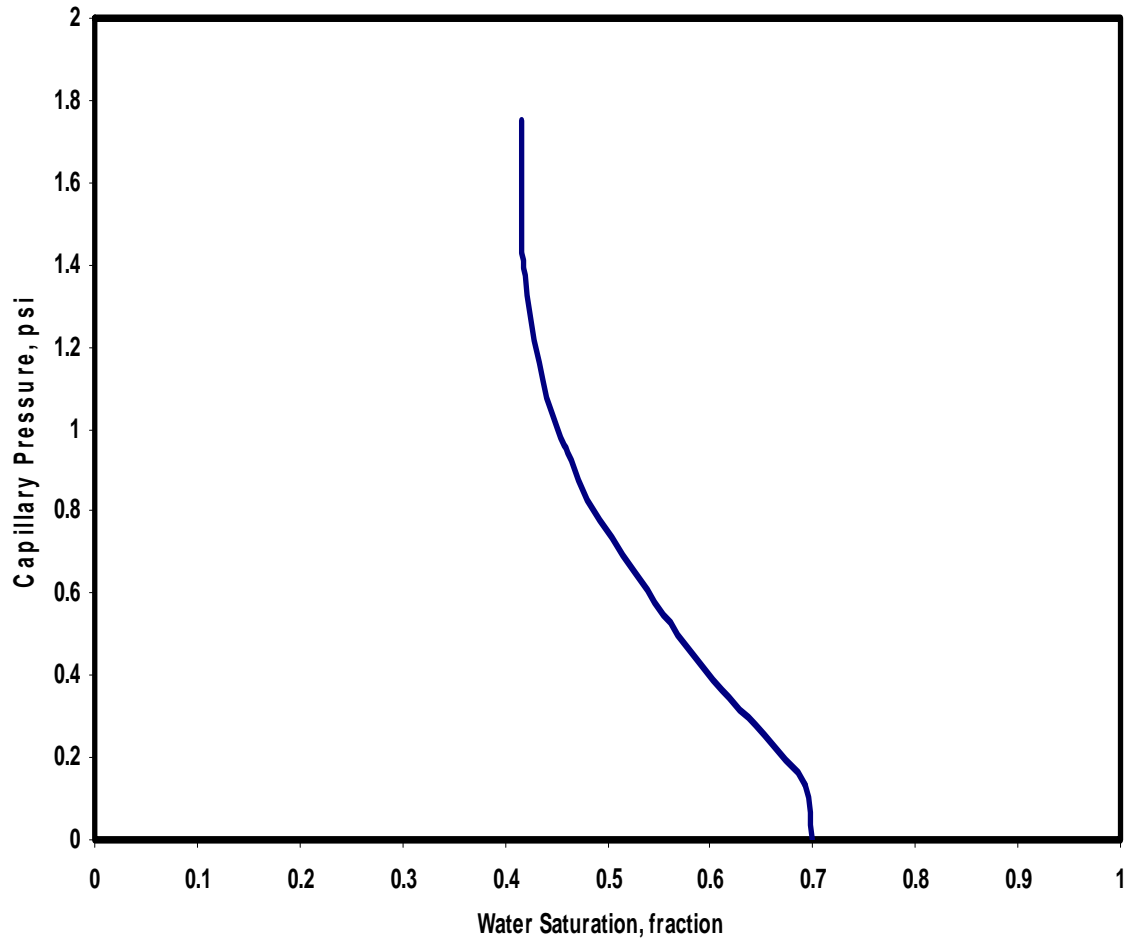
Fig. 4.4—Capillary pressure curve
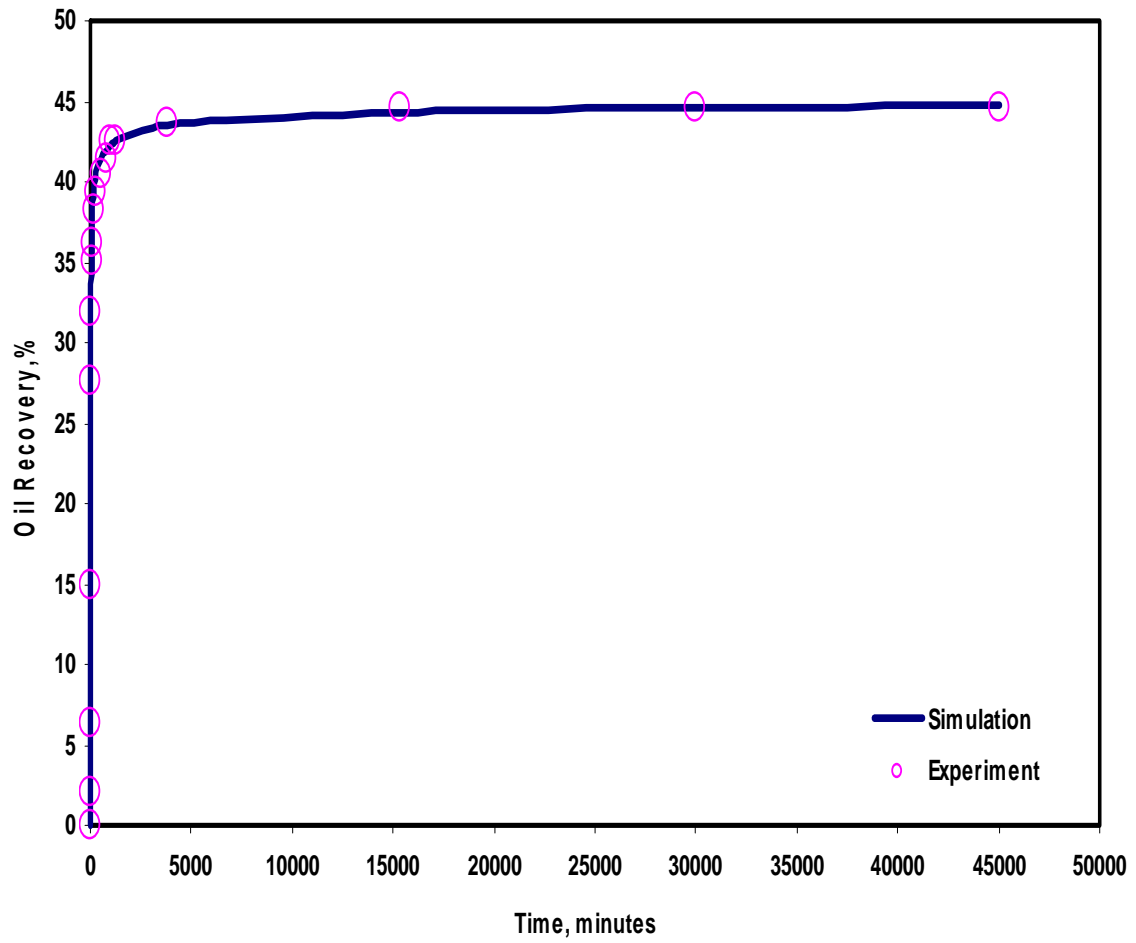
Fig. 4.5—Match of the simulated oil recovery with the observed oil recovery

The distance of the water imbibed into the core plug is demonstrated by the water saturation profile as shown in **Fig. 4.6.** As time increases, more water is imbibed into the core plug and, in turn, more oil is recovered.
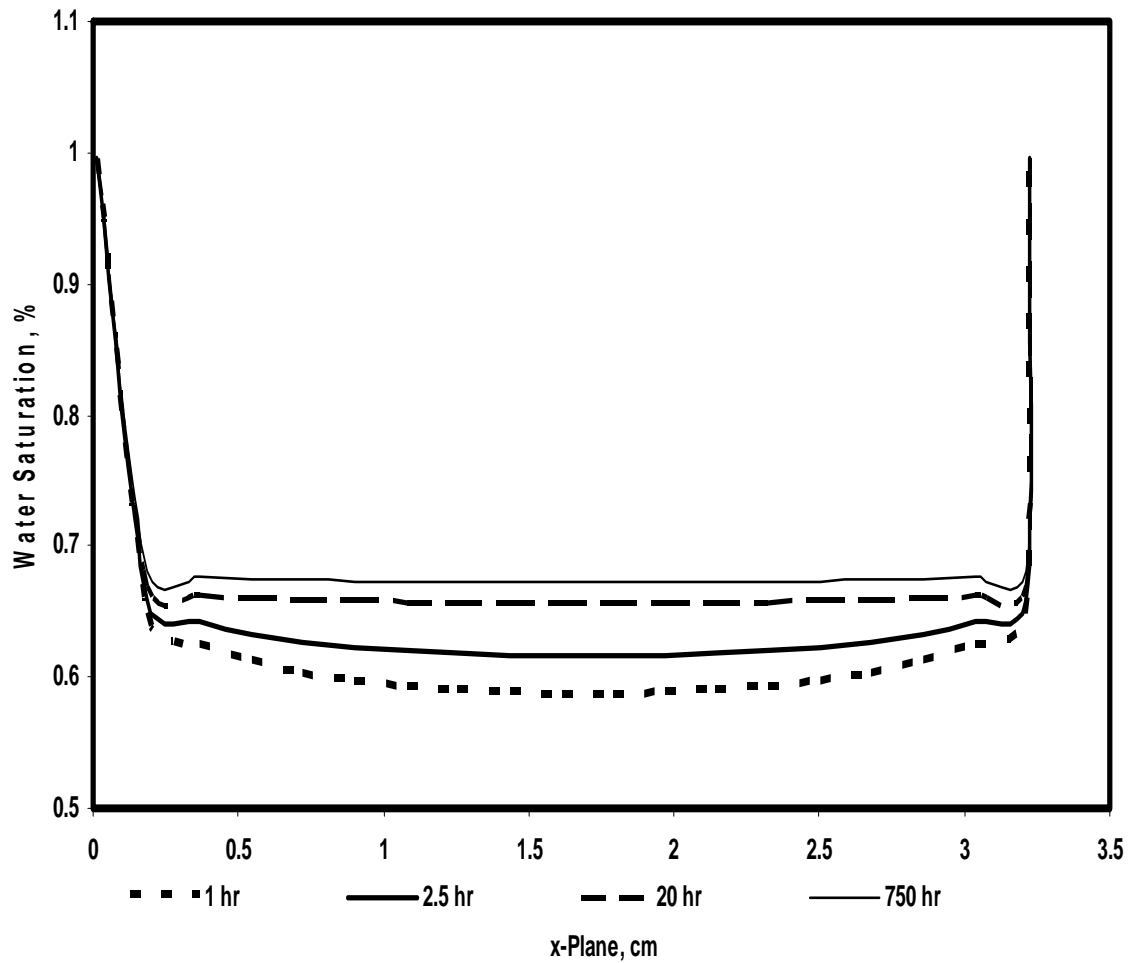
Fig. 4.6—Water distribution at different imbibition times from x-plane view

4.3 Boundary Conditions

Once the model has been satisfactorily built, different types of boundary conditions have been studied. Oil recoveries have been investigated for All Faces Open, Two Ends Open, Two Ends Closed, and One End Open types of spontaneous imbibition model.

4.3.1 All Faces Open (AFO)

The base case had "All Faces Open" type of boundary condition. This meant that all faces of the core were open to imbibition, i.e., a wetting phase imbibed into the core from all sides.

4.3.2 Two Ends Open (TEO)

"Two Ends Open" type of boundary condition has been applied to the base case model. This type of imbibition model refers to the matrix block with only two faces at the top and bottom open to imbibition. The sides of the core were closed for a wetting phase to imbibe. The boundary conditions for this model were as follows:

$$
\begin{aligned}
S_w(x,y,z,t) &= 1, x = 0 \\
S_w(x,y,z,t) &= 1, y = 0 \\
S_w(x,y,z,t) &= 1, x = L_x \\
S_w(x,y,z,t) &= 1, y = L_y
\end{aligned}
\qquad \text{..} \quad (4.2)
$$

4.3.3 Two Ends Closed (TEC)

"Two Ends Closed" type of boundary condition refers to the imbibition model with two impermeable faces at the top and the bottom. For this type of imbibition, the flow occurs simultaneously through four faces of the matrix block. The boundary conditions for this type of the model were as follows:

$$S_Z(x,y,z,t) = 1, z = 0$$
$$S_Z(x,y,z,t) = 1, z = L_Z$$

\.. (4.3)

4.3.4 One End Open (OEO)

"One End Open" type of boundary condition assumed that the imbibition occurred only through one face. In our case a wetting phase imbibed through the bottom of the core. The boundary conditions for OEO type of the model were as follows:

$$S_X(x,y,z,t) = 1, x = L_X$$
$$S_Y(x,y,z,t) = 1, y = L_Y$$

\.. (4.4)

The schematic representation of Two Ends Open, Two Ends Closed, and One End Open types of boundary conditions is shown in **Fig. 4.7**. In all cases a wetting phase was in contact with the core at all times. To account for this effect, a water saturation value of 1.0 was assigned to a very small extra gridblock. The water saturation of this gridblock was kept constant at all times. To achieve constant water saturation, decision was made to multiply the pore volume of gridblock by a big number.
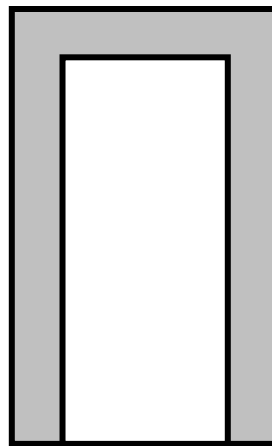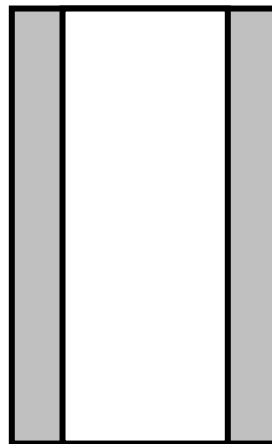
Fig 4.7— Schematic representation of imbibition in cores with different boundary conditions: A) One End Open, B) Two Ends Open, and C) Two Ends Closed types

4.4 The Effect of Gravity on Modeling of Imbibition Experiment

Even though the gravity has an effect on imbibition, in the current study the gravity effect was neglected, because the scope of the research covers only capillary imbibition, where capillary forces are dominant and gravity forces are neglected.

To neglect the effect of the gravity, the Bond number had to be adjusted. Bond number is the measure of the relative effect of the gravity forces to that of capillary forces. The expression for Bond number is as follows:

$$B_O = \frac{g(\rho_1 - \rho_2)H^2}{\sigma} ,$$ …………………………….....…… (4.5

where g is gravitational acceleration, ρ_1 and ρ_2 are the densities of a wetting and a non-wetting phase accordingly, H is the height of the core, and σ is surface tension. When B_o >>1, capillarity is negligible, if B_o <<1, then gravity is negligible.

Although the height of the core was very small, it was decided to reduce the effect of the gravity by making density difference equal to zero. The density of water has been changed from 1 g/cm^3 to 0.8635 g/cm^3 and made equal to the density of oil. This way the value of Bond number has been set to zero, which meant that the gravity effect has been neglected.

Fig. 4.8 shows the effect of the gravity on oil recovery. From the figure it was observed that the gravity effect wasn't so prominent, and neglecting gravity didn't significantly affect the oil recovery.
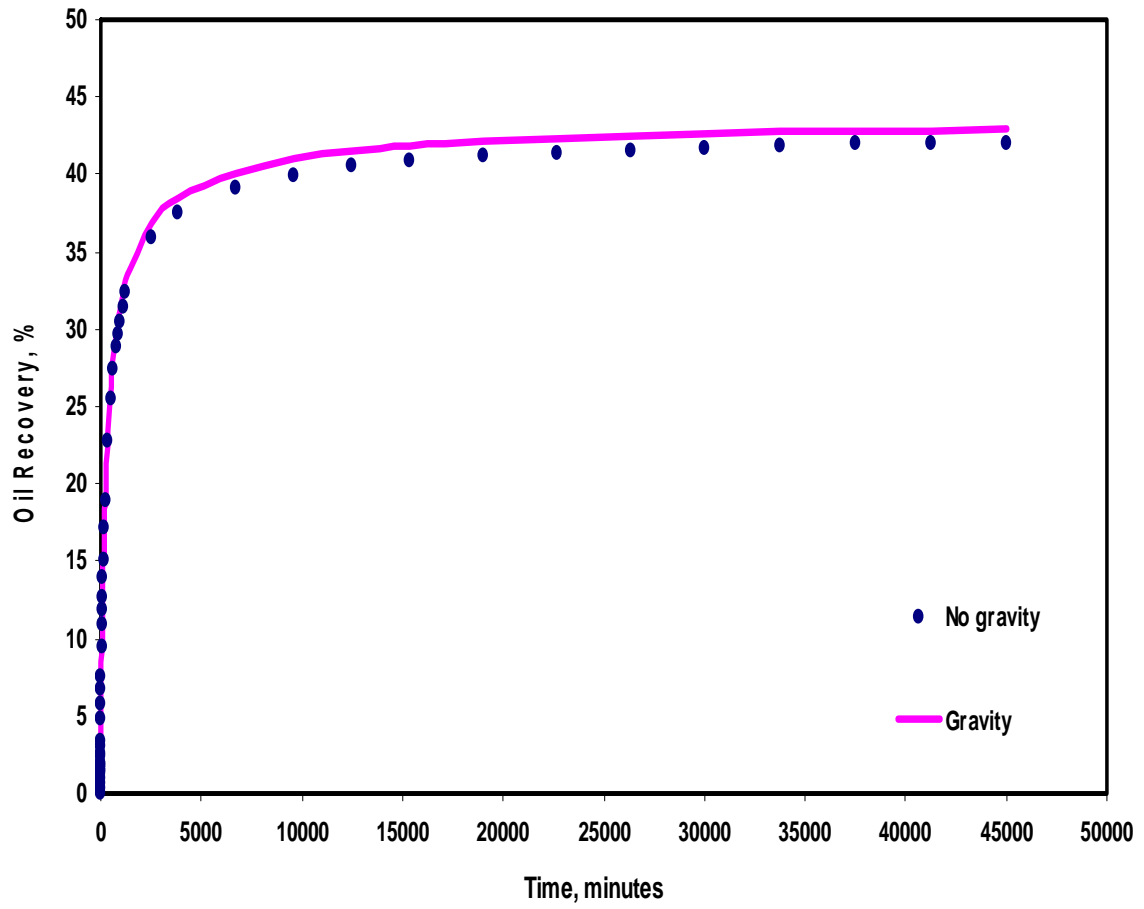
Fig 4.8—Effect of gravity on imbibition response

4.5 Comparison of Time Rates of Imbibition for Different Types of Boundary Conditions

The comparative study of time rates of spontaneous imbibition of water for different types of boundary conditions is presented here. The comparison was based on the total surface area available for imbibition and corresponding times taken for saturating a core until residual oil saturation. **Fig. 4.9** shows oil recovery curves for four types of boundary conditions: AFO, TEO, TEC, and OEO. As can be observed from the figure, the model with OEO type of boundary condition exhibits the smallest oil recovery, while the model with AFO type of boundary condition exhibits the largest value of oil recovery. The former type of boundary condition has only one face of the core available for imbibition, while the latter type of boundary condition has six faces of the core open for imbibition.

Fig. 4.10 is a plot of absolute time of imbibition as a function of the number of faces available for imbibition. It is observed from Fig. 4.10 that the time required for saturating a core with water until residual oil saturation increases exponentially, as the number of faces available for imbibition decreases. The comparison of all four types of boundary conditions shows that a non-wetting recovery for the AFO type of model is most efficient and fast, as compared with all other cases.
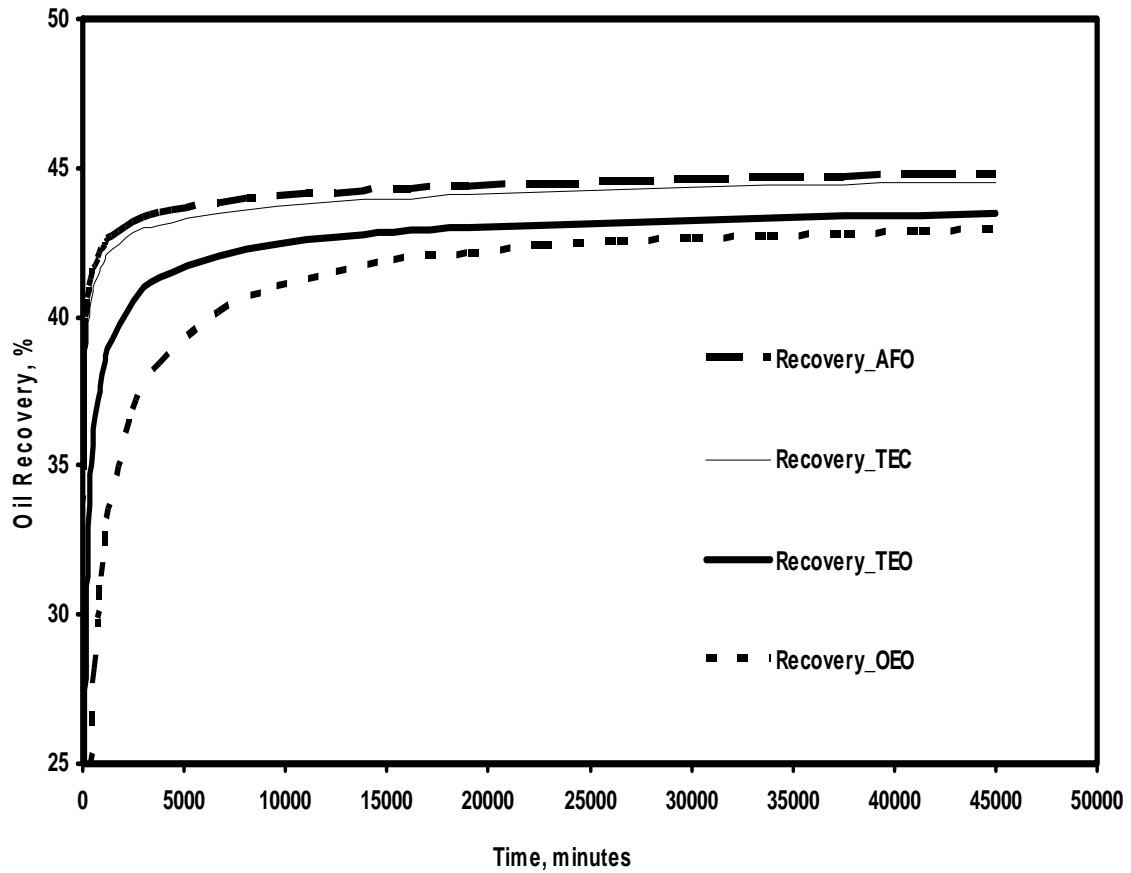
Fig 4.9—Oil recoveries for All Faces Open, Two Ends Closed, Two Ends Open, and One End Open types of boundary conditions
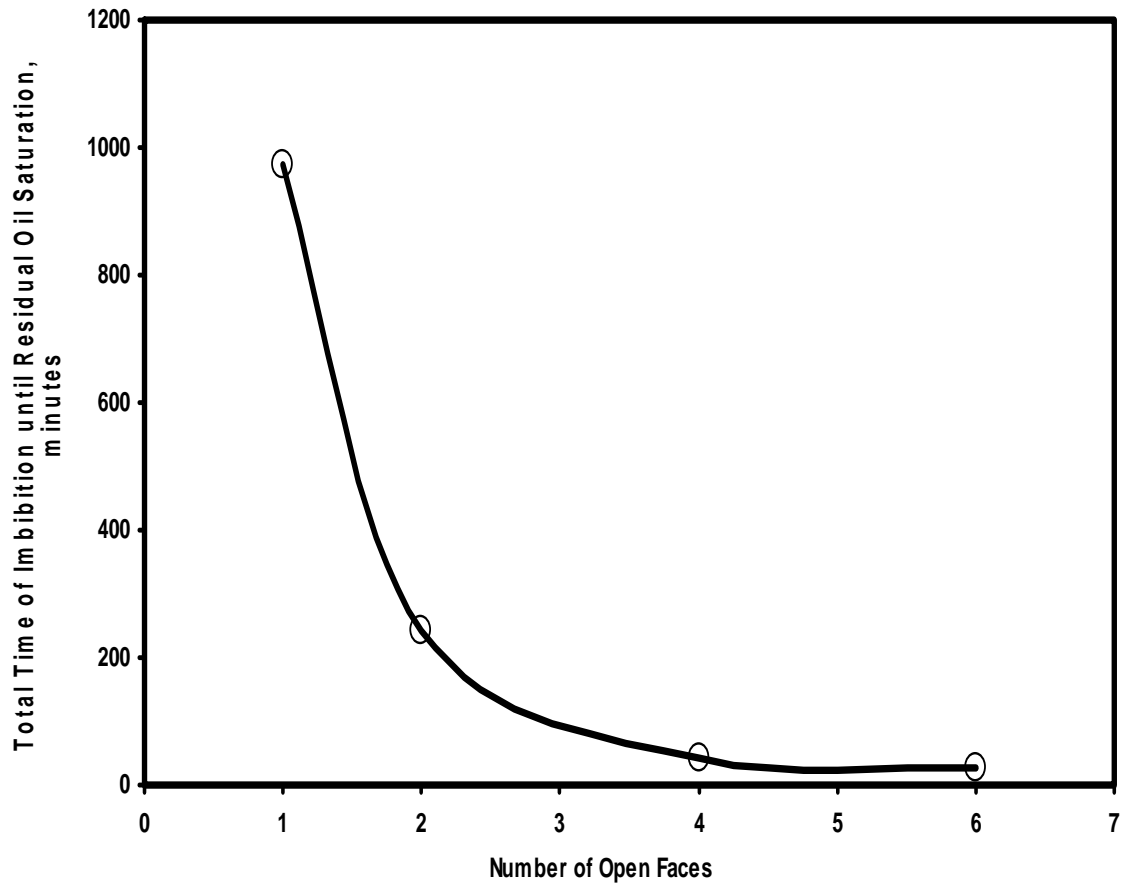
Fig 4.10—Absolute time for imbibition to reach S_{or} as a function of the faces available for imbibition

4.6 The Effect of Heterogeneity on the Imbibition Oil Recovery

The effect of heterogeneities on oil recovery has received limited treatment in the petroleum literature. The effect of varying permeability profiles along the core on oil recovery was investigated here. It is well known that under the influence of the capillary forces water imbibes from the more permeable zones of porous medium into the less permeable zones and displaces oil. However, without experimental or numerical studies it is difficult to determine oil displacement from the more permeable zone into the less permeable. The same problem could be brought up when water displaces oil from high permeable oil lenses into the less permeable zones of porous medium. For further investigation of the problem, numerical analyses have been performed.

4.6.1 Formulation of the Problem

To formulate the problem, a core with only one imbibing face open to fluid flow was considered. The permeability has been varied along the core. Particularly, two cases have been considered: the first case is when oil has been displaced by water and the permeability of the core was decreasing from the bottom to the top of the core; the second case is when permeability was increasing from the bottom to the top. A schematic of both cases is shown in **Fig. 4.11.** The core on the scheme has been conditionally divided into four parts for allowing a reader to understand the permeability change along the core. For the computational ease the permeability variance along the core was distributed linearly **Fig. 4.12.** This study was based on the numerical simulation, using the previously matched model of the spontaneous imbibition. The gravity effect was neglected.

The J–Function (Eq. 4.6) was used to scale capillary pressures to account for the differences in block permeability. The J-function has the effect of normalizing all

curves to approach a single curve. **Fig. 4.13** shows a J-curve, which was used a master curve and represented the permeability variance of the core (Fig.4.11)

$$J(S_w) = \frac{P_c}{\sigma \cos\theta}\sqrt{\frac{k}{\phi}}\ ,\quad \dots\dots\dots\dots\dots\dots\dots\dots\dots\dots\dots\dots\dots\dots \quad (4.6)$$

The results of numerical analyses are shown in **Fig. 4.14.** From the figure it was observed that oil recovery curves for both cases have generally known shape, but different oil recovery values. From the figure it is clear that capillary displacement of oil by water is more efficient for a case when water imbibes into the core in the direction of decreasing permeability.
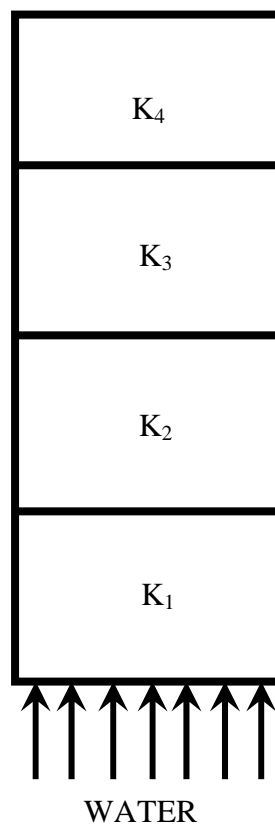
Fig 4.11—OEO imbibition model: first case-$k_1>k_2>k_3>k_4$ and second case-$k_1<k_2<k_3<k_4$
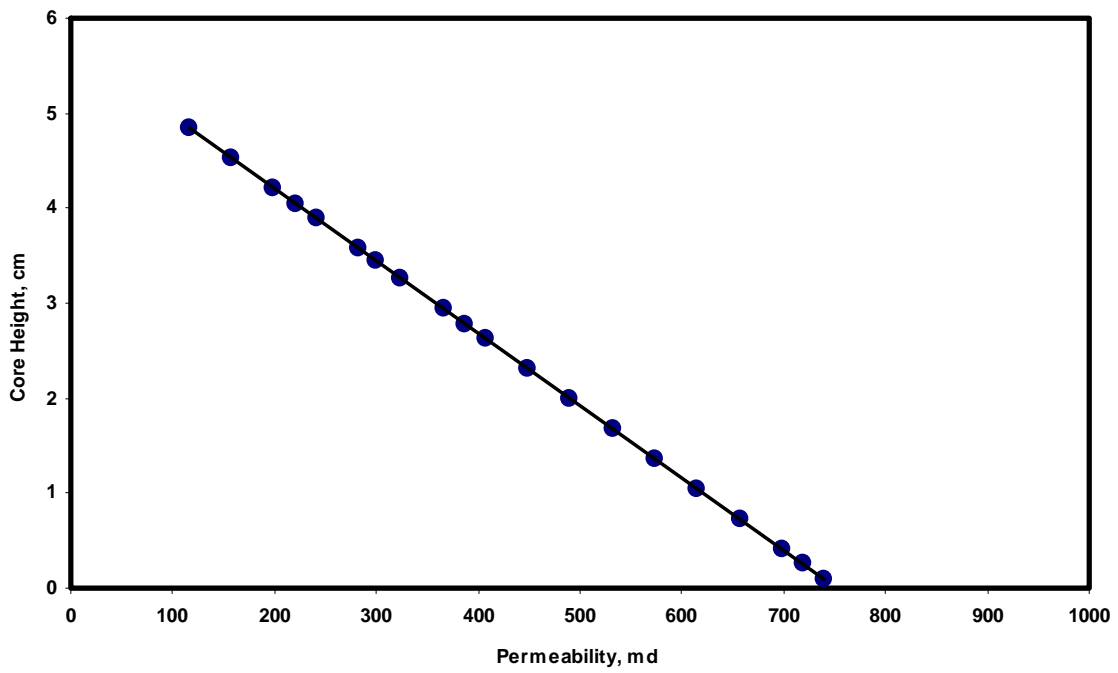
A)
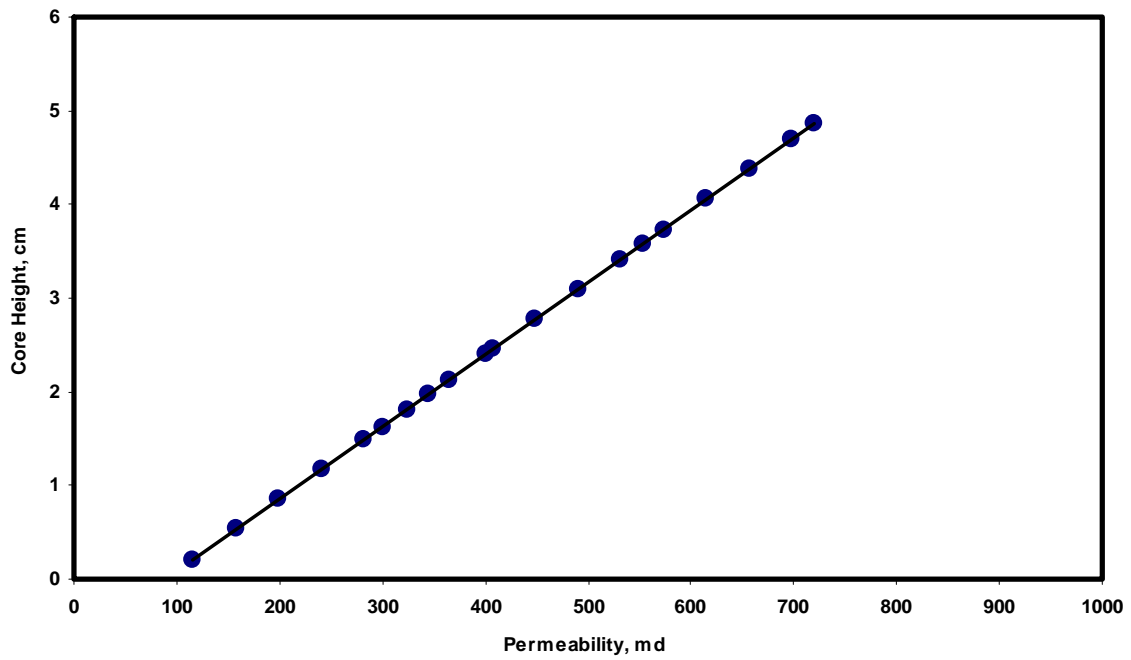
B)

Fig 4.12—Permeability profiles along the core: A) $k_1>k_2>k_3>k_4$,

B) $k_1<k_2<k_3<k_4$
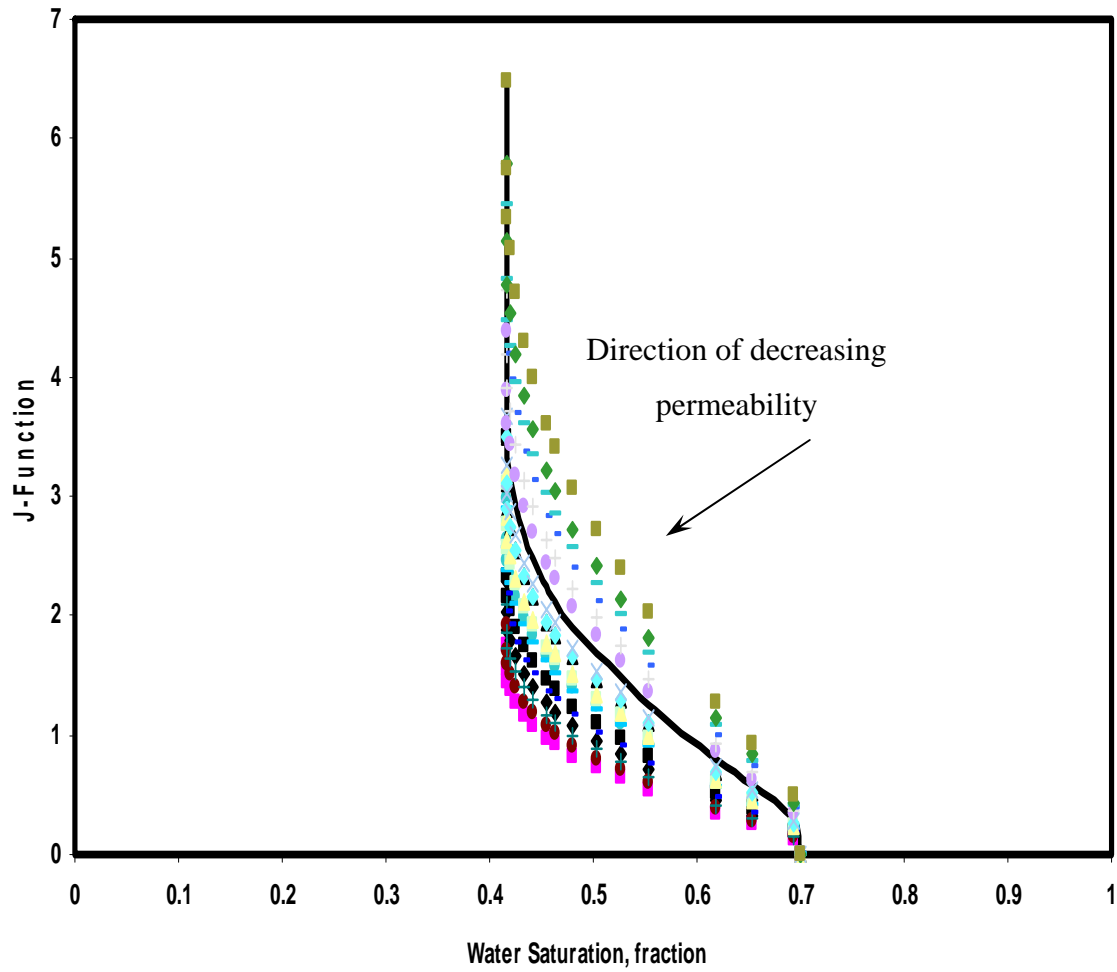
Fig 4.13— J-function correlation of capillary pressure data
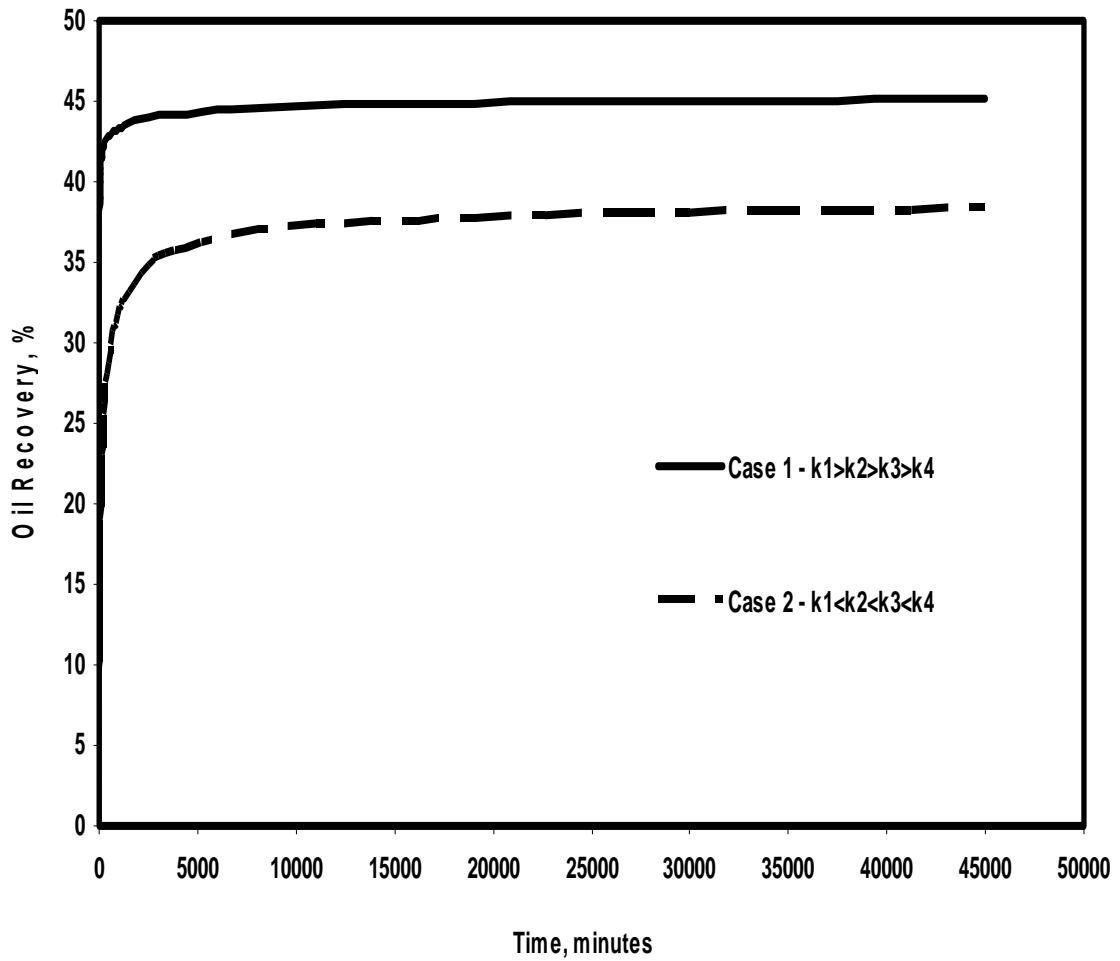
Fig 4.14— Oil recovery curves for different permeability profiles along the core

The explanation lies in understanding the mechanism of capillary displacement and also realizing that capillary pressure is an inversely proportional function of permeability, which means that when permeability decreasing the capillary pressure is increasing or vice-versa. So when water imbibes in the direction of decreasing permeability, it reaches the boundary of two different permeability zones and without any difficulty moves into the next zone. This unhampered movement occurs because water moves from the zones of low capillary forces into the zones with high capillary forces.

The case is different when the permeability of a porous medium increases in the direction of water imbibition. Water imbibed into the low permeable zone of the core moves ahead under the influence of capillary forces and, finally, reaches the boundary of the high permeable zone. At this point, the further movement of water is getting hindered because water moves into the zone with low capillary forces. So, the analyses indicated that oil displacement from a porous medium, consisting of the sequential zones of different permeabilities, is more efficient, if imbibition occurs in the direction of decreasing permeability than in the direction of increasing permeability.

4.7 Parametric Study

Capillary imbibition experiments usually take a long time, especially when we need to vary some parameters to investigate their effects. Therefore, a numerical modeling is needed to simulate this process.

This parametric study was based on the numerical simulation, using the previously matched model of the spontaneous imbibition. The gravity effect was neglected. The first series of computer runs were conducted to study the change in imbibition recovery, which was expected with the change in viscosities of the reservoir fluids.

The second series considered the changes caused by different capillary pressure and relative permeability curves. The third set of computer runs was conducted to examine oil recoveries for the models with different fracture spacing. Other reservoir and fluid properties were held constant.

4.7.1 The Effect of Water-Oil Viscosity Ratio

Fluid viscosity can significantly affect the rate of imbibition. The effect of different water-oil viscosity ratios, at which water imbibed into the core, was examined. The original water-oil ratio used in the base case model was 0.68:3.52. To examine the effect of oil viscosity on imbibition oil recovery, the simulation runs were made for two different oil viscosities: 0.352 and 50 cp. The water viscosity was held constant at 0.68 cp. The first case with 0.68:0.352 water-oil viscosity ratio simulated the case with favorable fluid flow mobility. The second case with 0.68:50 water-oil viscosity ratio simulated the case with unfavorable fluid flow mobility.

The effect of different oil viscosities on the oil recovery for AFO type of spontaneous imbibition model is shown in **Fig. 4.15**. From the figure it can be observed that the lower the oil viscosity, the bigger the volumes of oil produced from the core as a function of time.

The distance of water imbibed into the core plug is demonstrated by the water saturation profile in **Fig. 4.16.** As oil viscosity increases, less and less water is imbibed into the core plug. Exactly the same picture has been observed with three other types of imbibition models.
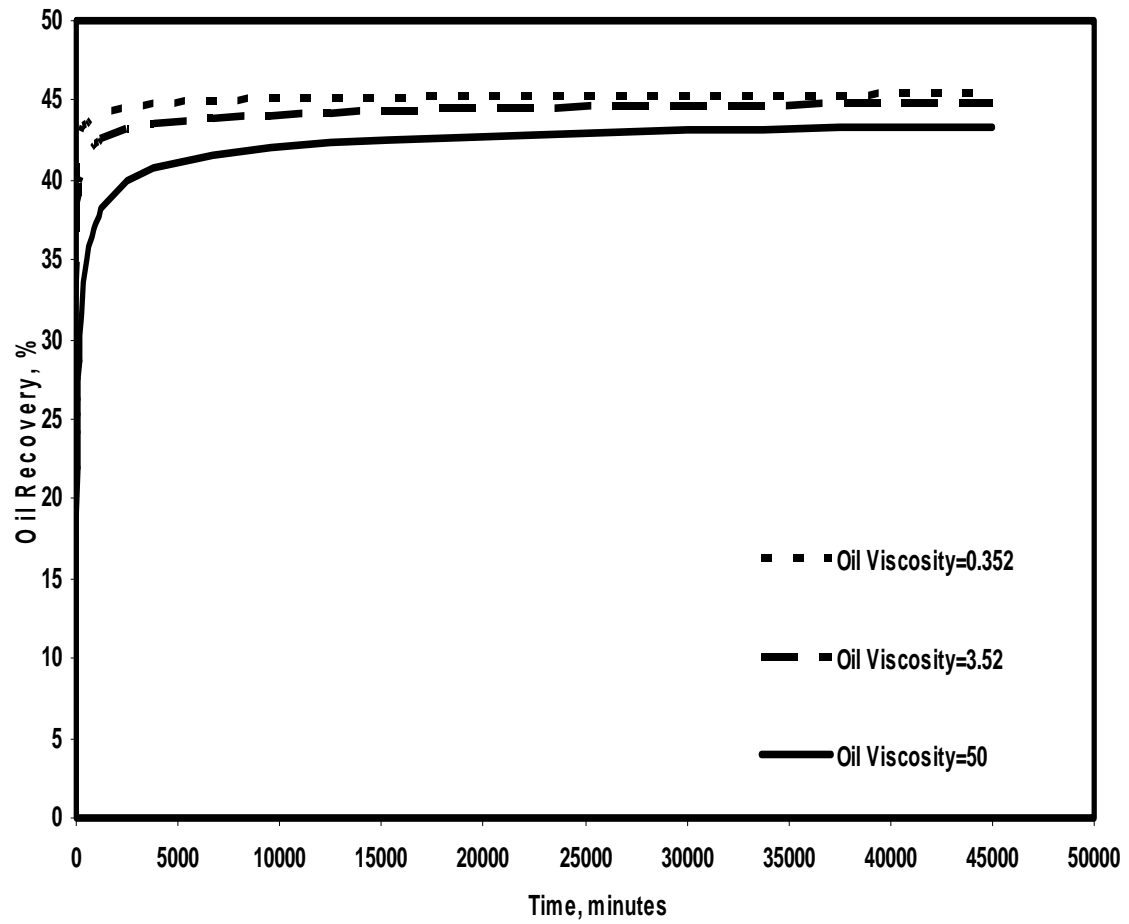
Fig 4.15— Oil recovery curves with different oil viscosities
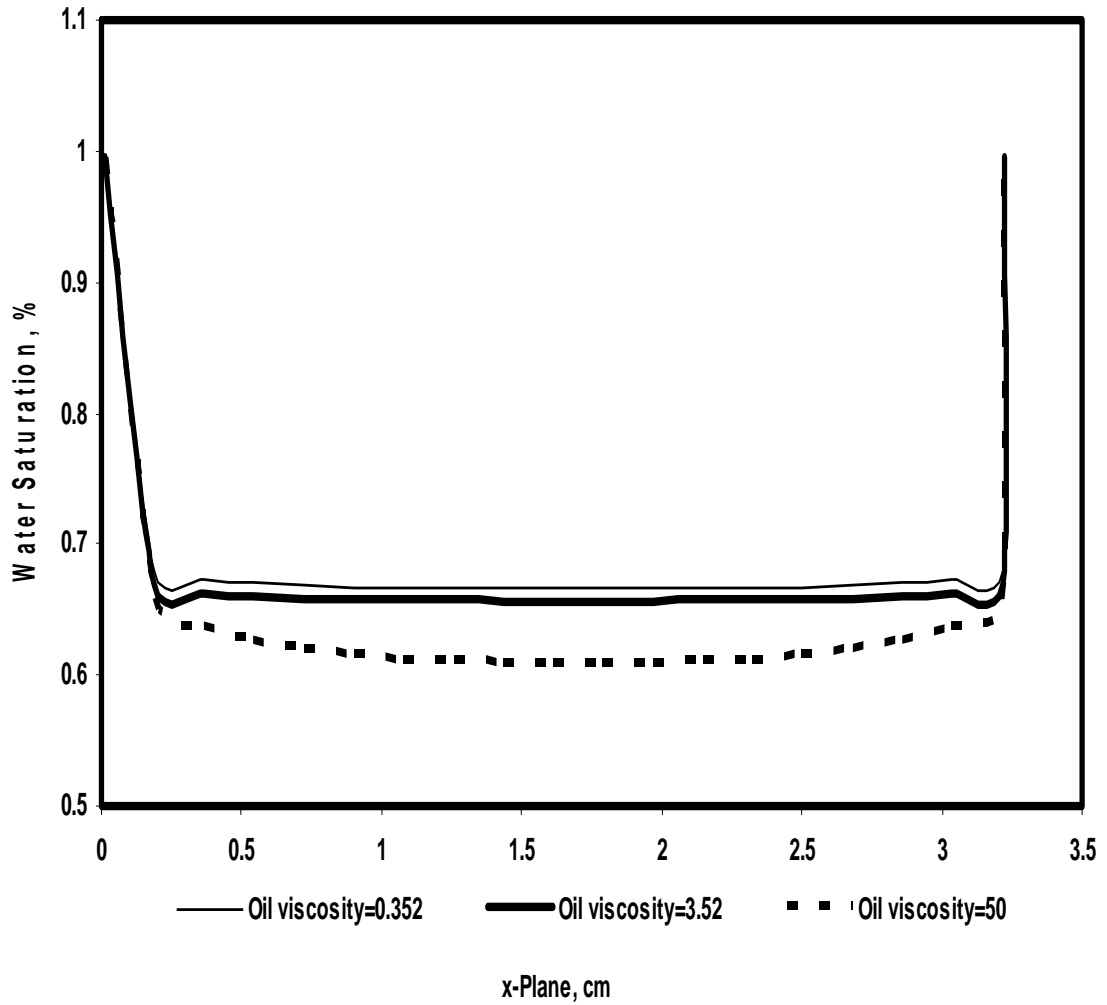
Fig 4.16— Water distribution at different oil viscosities

4.7.2 The Effect of Capillary Pressure and Relative Permeability

Capillary pressure is a function of pore sizes and the interfacial tension between the fluids in the matrix and the driving force during spontaneous imbibition. In general, the smaller the pore size or the higher the interfacial tension, the stronger the capillary pressure.

To investigate the sensitivity of imbibition capillary pressure on the imbibition oil recovery, two different capillary pressures were used with the multiplication in order of 0.1 and 10 to the matching results of capillary pressure. In other words, these series of simulation runs were made to determine the effect on imbibition of changing capillary pressure. AFO type of the spontaneous imbibition model was used. Other data used in the simulator remained unchanged.

Table 4.4 shows the capillary pressures for the Base Case and two test cases, namely Case 1 and Case 2. Changes in the imbibition oil recovery for these cases are clearly demonstrated in **Fig. 4.17.** It can be seen that the change from the Base Case to Case 1 caused a decrease in the oil recovery. Also, the change of capillary pressure from the Base Case to Case 2 caused an increase in spontaneous imbibition oil recovery.

Table 4.4—Capillary Pressure Values

Base Case Capillary Pressure, Psi	Case 1 Base Case P_C x 0.1, psi	Case 2 Base Case P_C x 10, psi
1.7537	0.1754	17.537
1.555	0.1555	15.55
1.445	0.1445	14.45
1.373	0.1373	13.73
1.273	0.1273	12.73
1.164	0.1164	11.64
1.078	0.1078	10.78
0.976	0.0976	9.76
0.922	0.0922	9.22
0.828	0.0828	8.28
0.733	0.0733	7.33
0.651	0.0651	6.51
0.547	0.0547	5.47
0.345	0.0345	3.45
0.254	0.0254	2.54
0.134	0.0134	1.34
0	0	0
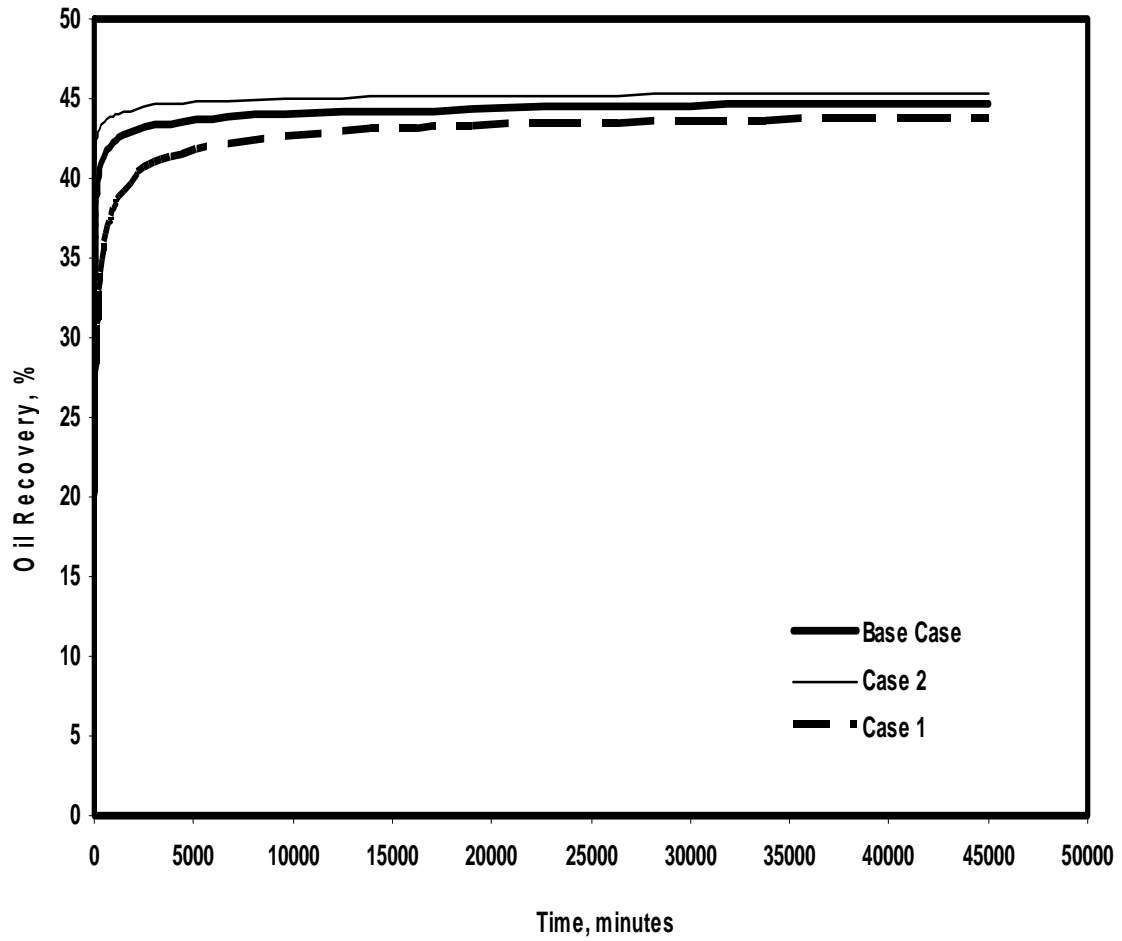
Fig 4.17— Effect of different capillary pressure on oil recovery

Capillary pressure is assumed to be the only driving force in the spontaneous imbibition process. Thus, increasing the capillary pressure increased the imbibition recovery as shown in Fig 4.17. Likewise, the decrease of imbibition oil recovery from the Base Case to Case 1 was also based on the fact that capillary pressure of Case 1 was lower than that of the Base Case.

To investigate the sensitivity of relative permeability curves on the imbibition oil recovery, two cases have been investigated. Relative permeabilities were multiplied in order of 0.1 and 0.5 to the matching results of relative permeability.

The results in **Fig. 4.18** and **Fig. 4.19** show that oil recovery by imbibition is sensitive to the oil relative permeability curves, while no significant effect was observed in changing the water relative permeability curves. The imbibition oil recovery was sensitive to the oil relative permeability. This can be explained by the fact that a capillary diffusion coefficient is a function of the square of oil relative permeability and, thus, affects the imbibition process much stronger.
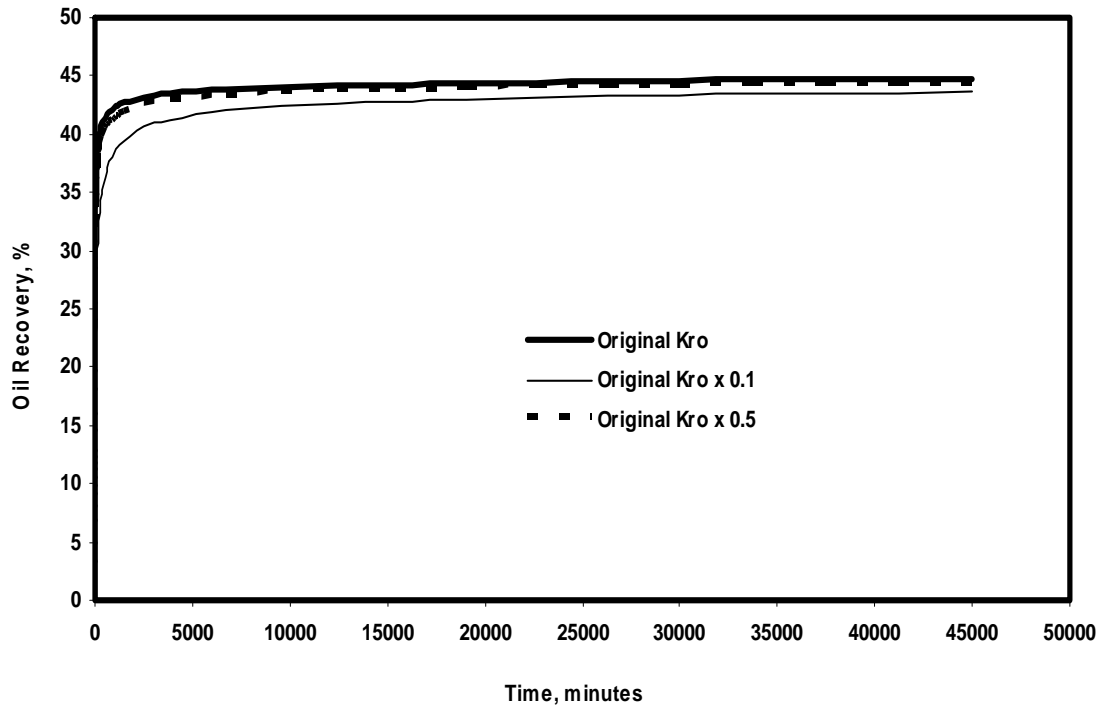
Fig 4.18— Effect of different oil relative permeabilities on oil recovery
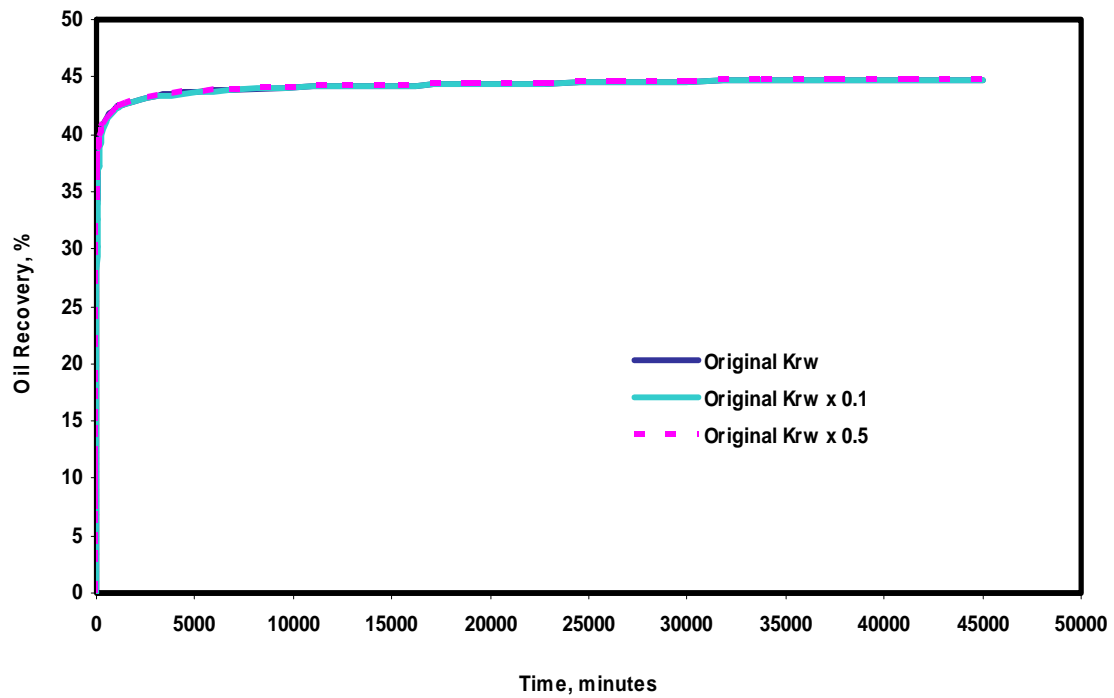
Fig 4.19— Effect of different water relative permeabilities on oil recovery

4.7.3 The Effect of Fracture Spacing

Here the effect of different fracture spacing has been investigated on the Two Ends Open type of model. Fracture spacing is the distance between parallel fracture planes. The top and the bottom of the model, which were open to water imbibition, have been assumed as fracture planes and the distance between the top and the bottom of the model has been varied to study the effect on oil recovery. Different fracture spacing has been obtained by multiplying original fracture spacing by 2, 4, and 8.

Fig. 4.20 and **Fig. 4.21** present a comparative study of time rates of spontaneous imbibition of water for different fracture spacing. The comparison here was based on the fracture spacing and the corresponding times taken to saturate the core until residual oil saturation. Fig. 4.20 shows oil recovery curves for four different fracture spacings.

Fig. 4.21, which is a plot of absolute time of imbibition as a function of the fracture spacing, points out that the time required for saturating a core with water until residual oil saturation increases linearly, as the fracture width increases.

Fig 4.20— Effect of different fracture spacing on oil recovery
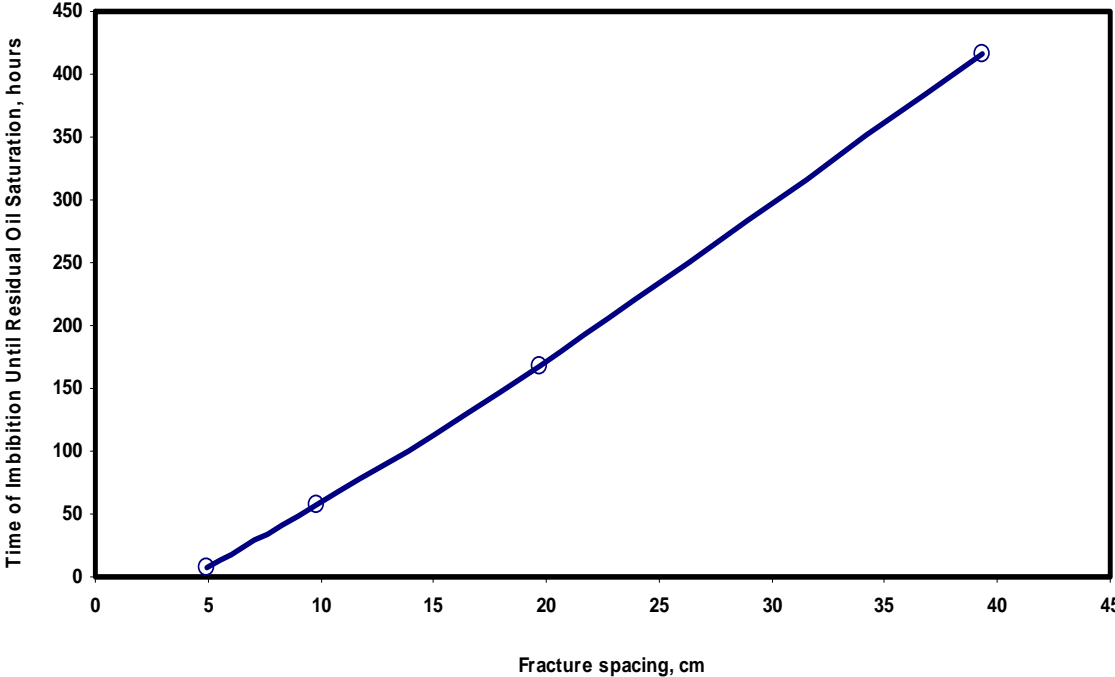
Fig 4.21— Absolute time for imbibition to reach S_{or} as a function of the fracture spacing

4.8 Summary and Discussions

In this chapter a numerical modeling of spontaneous imbibition experiment has been performed. Grid sensitivity analysis revealed optimal grid size, which has been used in the numerical studies. To improve the reservoir simulation data, the simulated oil recovery has been matched with observed oil recovery. The match was obtained by trial and error estimates of relative permeability and capillary pressure. Once the model has been satisfactorily matched, four types of boundary conditions have been investigated. They are All Faces Open, Two Ends Open, Two Ends Closed, and One End Open types of spontaneous imbibition model. The assumption that the gravity effect is negligible was made by setting the density of a wetting phase equal to the density of a non-wetting phase.

Numerical studies have been conducted to understand the displacement of oil by water. The comparative study of time rates of water spontaneous imbibition for different types of boundary conditions revealed the fact that the time required for saturating a core with water until residual oil saturation increases exponentially, as the number of faces available for imbibition decreases. The comparison of all four types of boundary conditions showed that oil recovery for the AFO type of a model is most efficient and fast compared with all other cases. The effect of varying permeability profiles along the core on oil recovery was investigated. Results showed that when water imbibes in the direction of decreasing permeability, oil recovery is higher than when water imbibes in the direction of increasing permeability.

The study of the effect of different water-oil viscosity ratios, at which water imbibed into the core, showed that the lower the oil viscosity, the bigger the volumes of oil produced from the core as a function of time. The series of simulation runs were made to determine the effect on imbibition of changing capillary pressure and water/oil relative permeabilities. The results showed that

increasing the capillary pressure increased the imbibition recovery. Oil recovery by imbibition was sensitive to the oil relative permeability curves, while no significant effect was observed in changing the water relative permeability curves.

A comparative study of time rates of spontaneous imbibition of water for different fracture spacing has been conducted. The results evinced the fact that the time required for saturating a core with water until residual oil saturation increased linearly, as the fracture width increased.
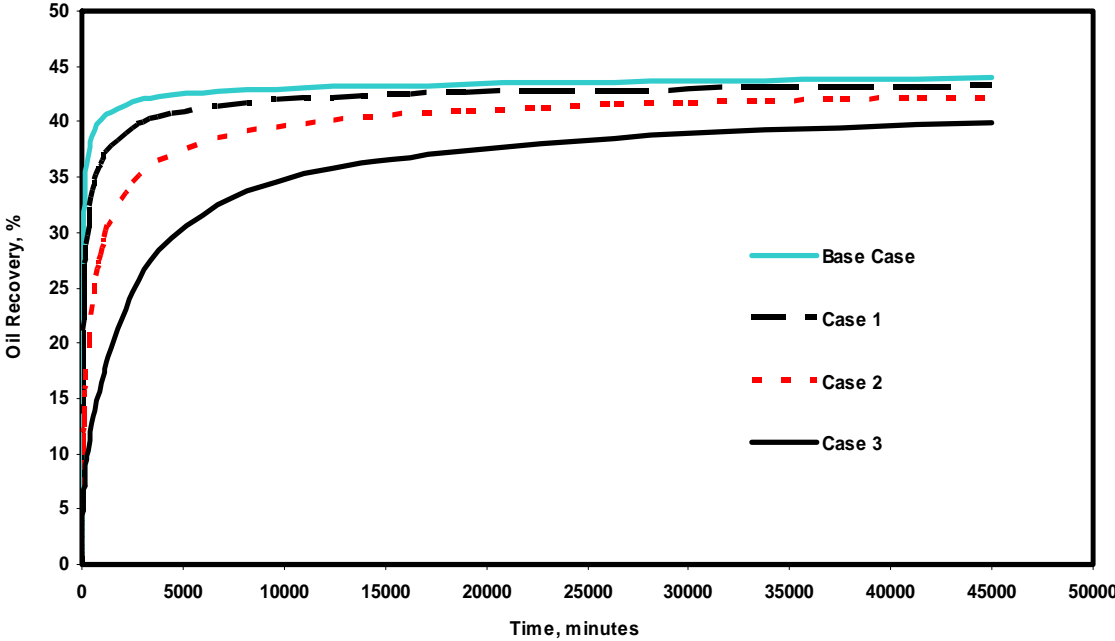
CHAPTER V

SCALING OF STATIC IMBIBITION MECHANISM

In this chapter, the static imbibition results from the previous chapter have been upscaled to the field dimensions. The validity of the new definition of characteristic length used in the modified scaling group has been evaluated. The new scaling group used to correlate simulation results has been compared to the early upscaling technique.

5.1 Scaling of Static Imbibition Data

Spontaneous imbibition is an important phenomenon in oil recovery from fractured reservoirs, where the rate of mass transfer between the rock matrix and the fractures determines the oil production. Imbibition is also important in evaluation of wettability of fluid/liquid/porous media system. The rate of imbibition depends primarily on the porous media, the fluids, and their interactions. These include relative permeabilities, matrix shapes, boundary conditions, fluid viscosity, interfacial tension (IFT), and wettability. Laboratory results need to be scaled to estimate oil recovery from the reservoir matrix blocks that have shapes, sizes, and boundary conditions different from those of the laboratory core samples. Upscaling of imbibition oil recovery from the small reservoir core sample allows us to predict field performance.

The basic requirements for scaling laboratory data to field conditions were investigated by Rapoport. In scaling imbibition results for different oil/brine/rock systems or in predicting field performance from laboratory measurements, Mattax and Kyte proposed the following scaling group:

$$t_D = t \sqrt{\frac{k_m}{\phi} \frac{\sigma}{\mu_W} \frac{1}{L^2}} \;,\; \dots\dots\dots\dots\dots\dots\dots\dots\dots\dots\dots\dots\dots\dots \quad (5.1)$$

where t_D is dimensionless time, t is imbibition time, k_m is matrix permeability, ϕ is porosity, σ is IFT, μ_w is water viscosity, and L is core length. The assumptions made in deriving this equation were that the sample shapes must be identical, the oil/water viscosity ratio must be duplicated, the gravity effects must be neglected, initial fluid distribution must be duplicated, the capillary pressure functions must be related by direct proportionality, and the relative permeability functions must be the same.

In oil production from fractured reservoirs, the systems with different matrix sizes, shapes, and boundary conditions will give different mass transfer rates between the fractures and the rock matrix. The smaller the ratio of a volume to open surface area, the faster the imbibition rate. So, based on the work of Mattax and Kyte and Kazemi *et al.* a characteristic length was proposed by Ma *et al.*, which was defined as follows:

$$L_C = \sqrt{\frac{V}{\sum\limits_{i=1}^{n} \frac{A_i}{x_{Ai}}}} \;,\; \dots\dots\dots\dots\dots\dots\dots\dots\dots\dots\dots\dots\dots\dots \quad (5.2)$$

where V is the bulk volume of the matrix, A_i is the area open to the imbibition at the ith direction and x_{Ai} is the length defined by the shape and boundary conditions of the matrix block. Because one of the assumptions in deriving Eq. 5.1 is that viscosity ratios are identical, Ma *et al.* also proposed to use oil viscosity in Eq. 5.1, provided that the viscosity ratio is constant, taking into consideration from the recent studies that for water/oil systems imbibition rate is proportional to the geometric mean of the water and oil phase viscosities,

$$\mu_g = \sqrt{\mu_O \mu_W} \;.\; \dots\dots\dots\dots\dots\dots\dots\dots\dots\dots\dots\dots\dots\dots \quad (5.3)$$

So, to account for both the effect of viscosity ratio and boundary conditions, the following modified scaling group was proposed by Ma *et al.*:

$$t_D = t \sqrt{\frac{k_m}{\phi}} \frac{\sigma}{\mu_g} \frac{1}{L_C^2} \; . \; \dots\dots\dots\dots\dots\dots\dots\dots\dots\dots\dots\dots\dots \quad (5.4)$$

5.1.1 Scaling Spontaneous Imbibition Mechanism with Different Types of Boundary Conditions

In the present work, the applicability of Eq. 5.4 was tested through extensive numerical study of the effect of boundary conditions. Two types of boundary conditions have been examined: One End Open and Two Ends Open. Then the results from numerical studies of spontaneous imbibition mechanism were used to compare between Eq 5.1 and Eq. 5.4. The comparison has been performed on the semi-log plot of oil recovery vs. dimensionless time.

Fig. 5.1 shows correlation of results for different boundary conditions using Eq. 5.1. **Fig. 5.2** shows correlation of results for different boundary conditions using characteristic length in Eq. 5.4. Comparison of both figures revealed the fact that points are more scattered in Fig. 5.1 than in Fig. 5.2. This fact proved that using characteristic length in the equation of dimensionless time improves the correlation for the models with different boundary conditions.
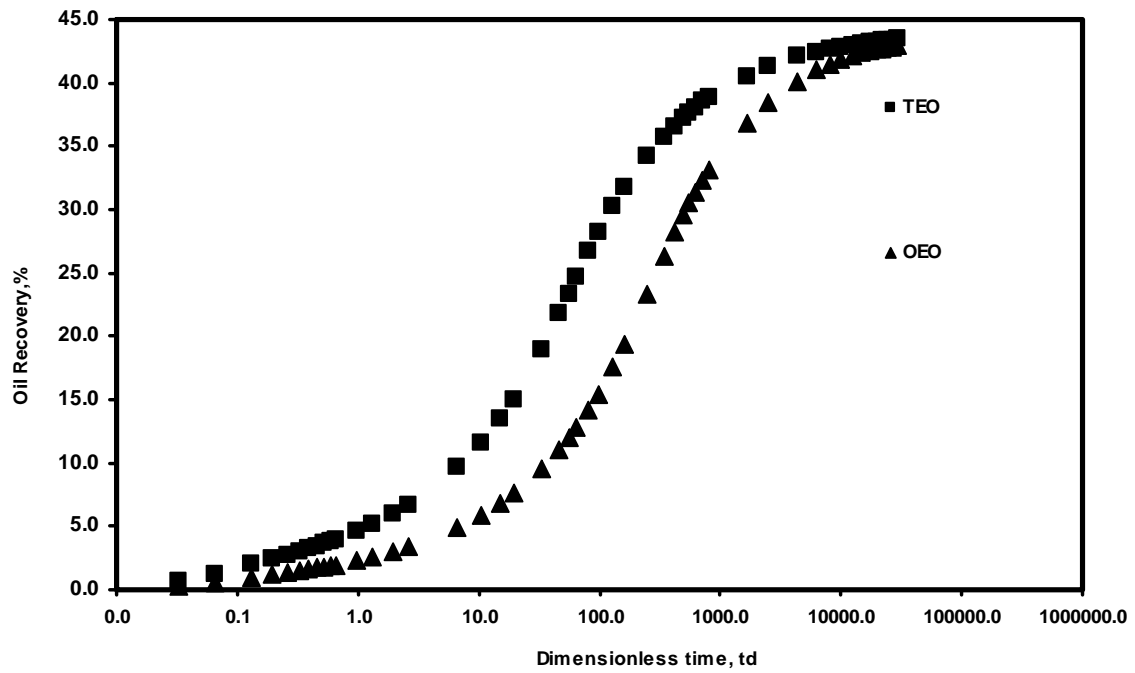
Fig 5.1— Correlation of the results for the systems with different boundary conditions, using the length of the core in the equation of dimensionless time
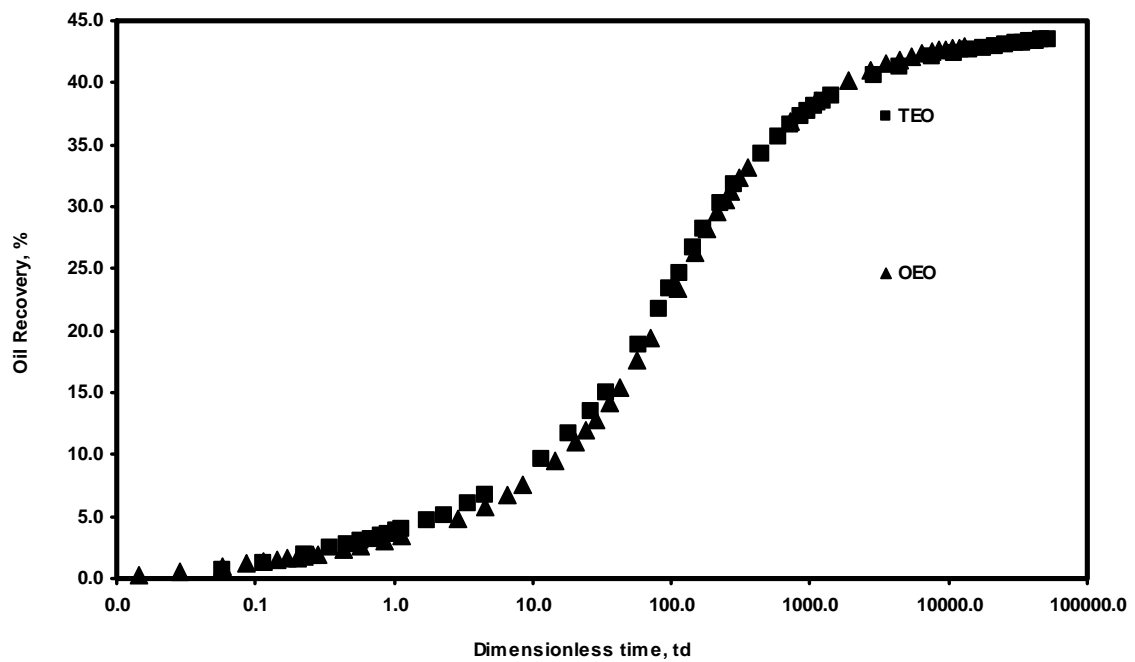
Fig 5.2— Correlation of the results for the systems with different boundary conditions, using the characteristic length in the equation of dimensionless time

5.1.2 Scaling Spontaneous Imbibition Mechanism with Varying Mobility Ratios

Here, the new scaling group proposed to correlate simulation results has been compared to the early upscaling technique. The previous scaling studies of spontaneous imbibition didn't pay too much attention to the varying mobilities of the fluids. Therefore, it was decided to study this effect and compare results from the previous upscaling technique (Eq. 5.4) to the results from the newly developed scaling equation.

The newly developed scaling technique has been proposed by Zhou *et al.*[45] They included characteristic mobilities of a wetting and a non-wetting phase into the equation of dimensionless time. The equation is as follows:

$$t_D = t\sqrt{\frac{k_m}{\phi}}\frac{\sigma}{L_C{}^2}\sqrt{\lambda_W \lambda_{NW}}\frac{1}{\sqrt{M}+\frac{1}{\sqrt{M}}} , \quad \ldots\ldots\ldots\ldots\ldots\ldots \quad (5.5)$$

$$\lambda = \frac{k}{\mu} , \quad \ldots\ldots\ldots\ldots\ldots\ldots\ldots\ldots\ldots\ldots\ldots\ldots\ldots\ldots\ldots\ldots \quad (5.6)$$

and,

$$M = \frac{\lambda_W}{\lambda_{NW}} , \quad \ldots\ldots\ldots\ldots\ldots\ldots\ldots\ldots\ldots\ldots\ldots\ldots\ldots\ldots \quad (5.7)$$

where λ is a characteristic mobility for a wetting and a non-wetting phase, and M is characteristic mobility ratio. Here, end-point relative permeabilities are used when calculating λ and M. The mobility ratios also depend on the viscosity of fluids. The above equation is valid, only if relative permeability and capillary pressure functions are similar for all of the measurements. **Fig. 5.3** and **Fig. 5.4** show comparison between the newly proposed upscaling method (Eq. 5.5) and previous upscaling technique (Eq. 5.4). The comparison is shown for two types of boundary conditions: Two Ends Open, and One End Open.
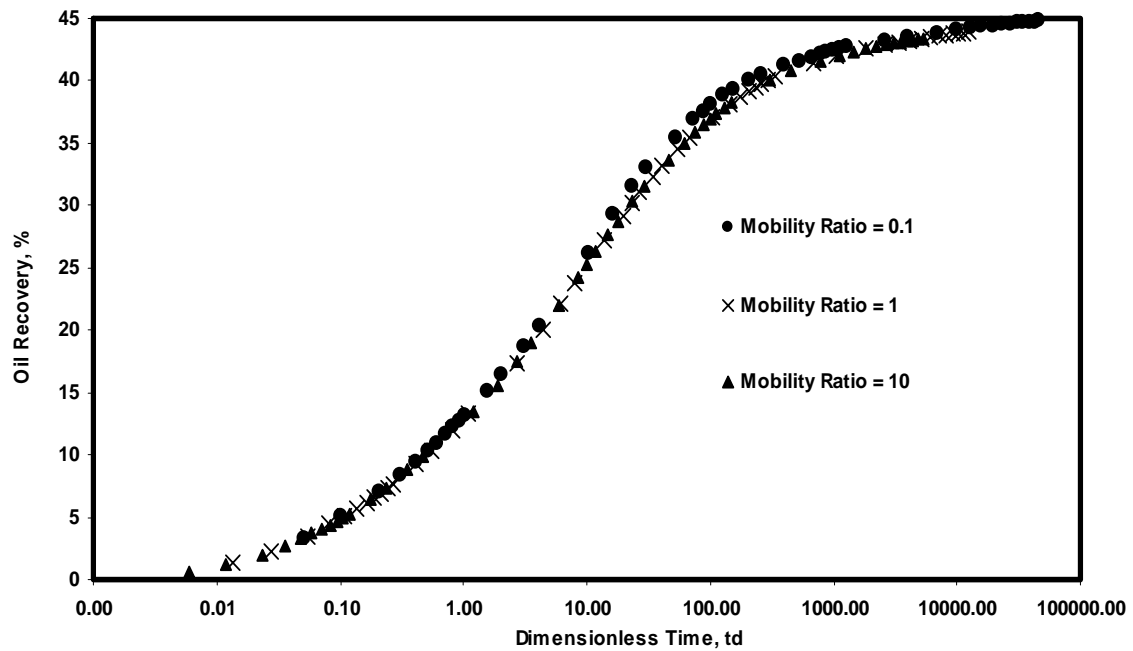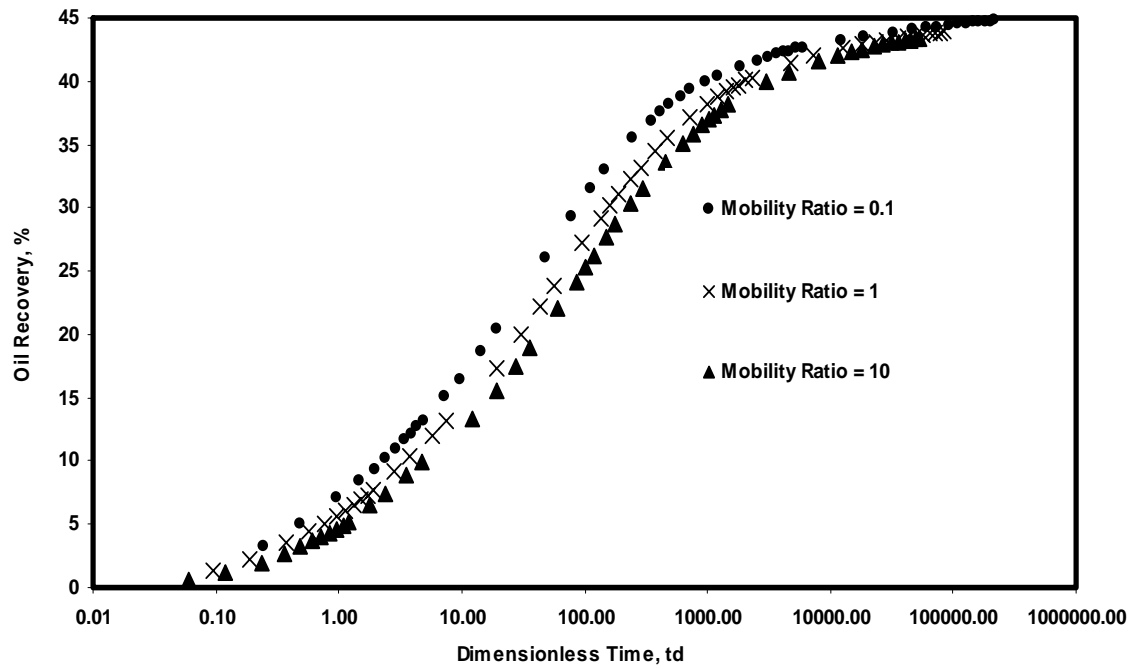
Fig 5.3— Comparing correlation of the results for the systems with different mobility ratios using Eq. 5.4 and Eq. 5.5 – Two Ends Open
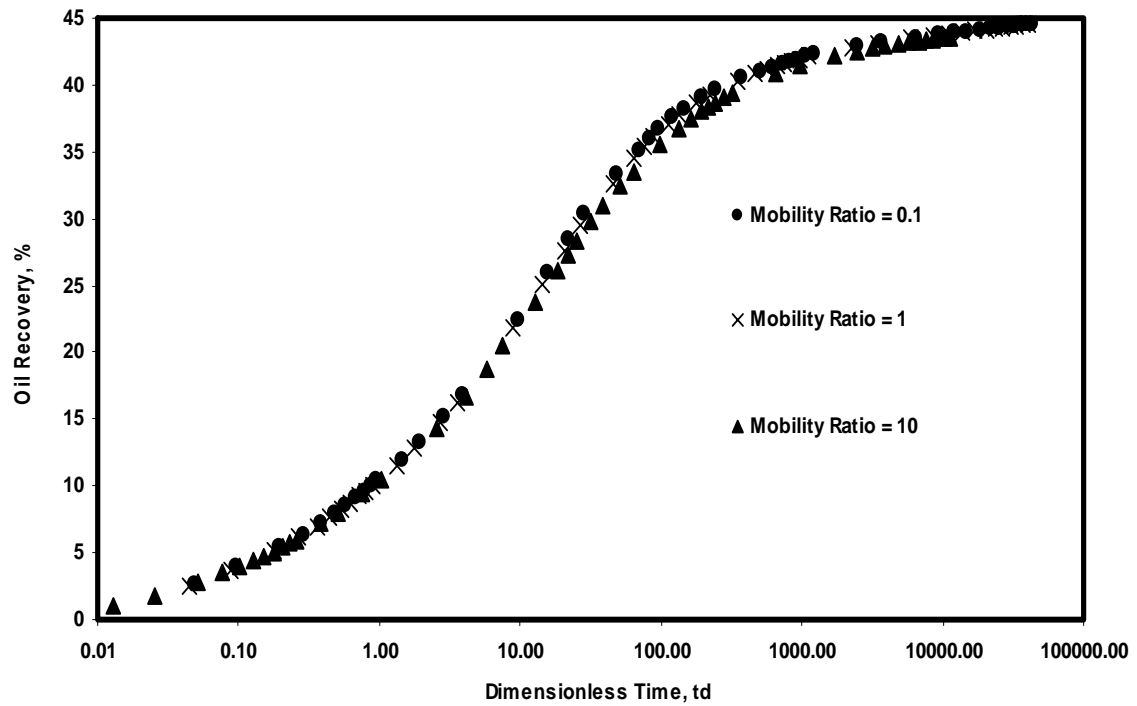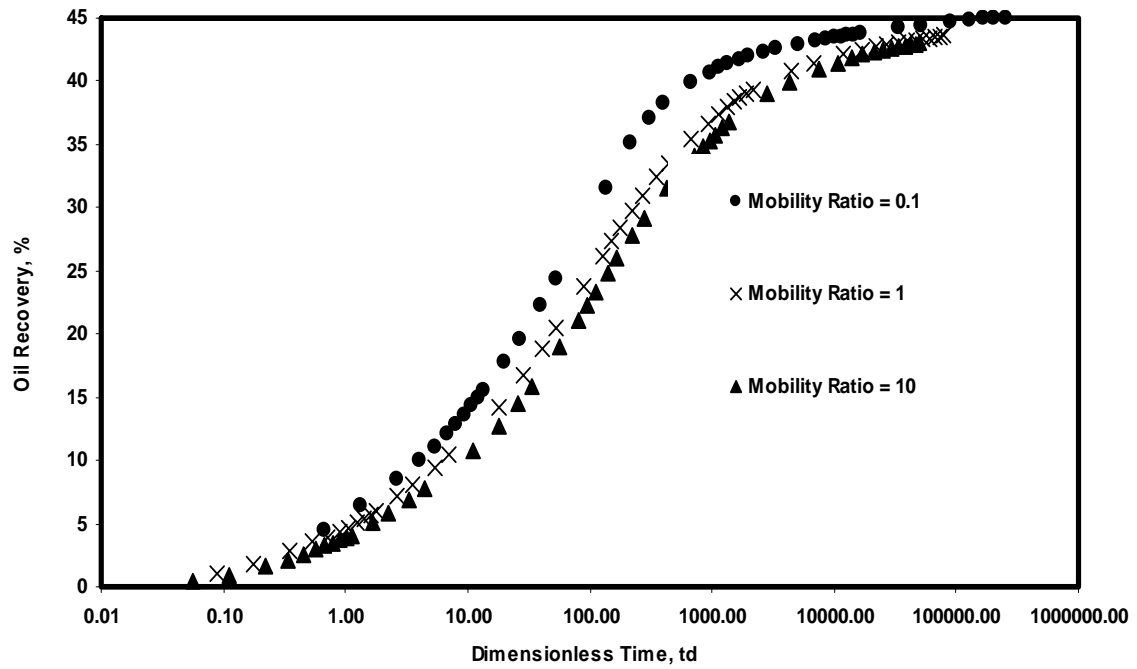
Fig 5.4— Comparing correlation of the results for the systems with different mobility ratios using Eq. 5.4 and Eq. 5.5 – One End Open

Three mobility ratios have been considered. The first case was with favorable mobility ratio, the second case was with unit mobility ratio, and the third case was with unfavorable mobility ratio. In all cases, oil viscosity has been altered, and water viscosity remained unchanged. From both figures it could be observed that the curves fall into a narrow range, when we use the newly developed scaling technique. The scaling is almost perfect with slight differences at late times. These differences, probably, result from the influence of the boundary of the porous medium on imbibition. When using a previous scaling equation, the data is more scattered.

So, we observe a pretty good correlation for the results of spontaneous imbibition with the new scaling technique. The recovery curves agree reasonably well for all mobility ratios. The data are reduced to a single curve in spite of the fact that non-wetting fluid viscosity varies by 3 orders of magnitude. The results indicate that the new dimensionless time can significantly improve the scaling of spontaneous imbibition.

5.2 Summary and Discussions

In this chapter, the spontaneous imbibition results from the previous chapter have been upscaled to the field dimensions. The validity of the new definition of characteristic length used in the modified scaling group has been evaluated. The new scaling group used to correlate simulation results has been compared to the early upscaling techniques.

The results revealed the fact that the characteristic length in the equation of dimensionless time improves a correlation between data points for the models with different boundary conditions. The new scaling technique, which was used for upscaling, significantly improved correlations by taking end-point fluid phase mobilities and the

mobility ratios into account. The comparison between the new and the previous dimensionless times proved that even if non-wetting fluid viscosity varies by 3 orders of magnitude, the data could be reduced to a single curve, if we use new dimensionless time definition.

CHAPTER VI

SUMMARY AND CONCLUSIONS

In the current work, the different aspects of spontaneous imbibition have been studied. Spontaneous imbibition is a process, where capillary forces are dominant. Capillary imbibition, in the petroleum literature, is described as a spontaneous penetration of a wetting phase into a porous media, while displacing a non-wetting phase by means of capillary pressure.

Capillary imbibition experiments usually take a long time, especially when we need to vary some parameters to investigate their effects. Therefore, to achieve objectives of the present study, numerical modeling of spontaneous imbibition experiment was performed using a two-phase black-oil commercial simulator (CMG™). The experimental results from water static imbibition experiments performed in the laboratory have been obtained. Grid sensitivity analysis revealed optimal grid size, which has been used in further numerical studies. To improve the reservoir simulation data, the simulated oil recovery has been matched with observed oil recovery. The match was obtained by trial and error estimates of relative permeability and capillary pressure. Once the model has been satisfactorily matched, four types of boundary conditions have been investigated. They are All Faces Open, Two Ends Open, Two Ends Closed, and One End Open types of spontaneous imbibition model. The assumption that the gravity effect is negligible was made by setting the density of a wetting phase equal to the density of a non-wetting phase. Numerous parametric studies have been performed and the results were analyzed in detail to investigate oil recovery during spontaneous imbibition with different types of boundary conditions. These studies included the effect of

varying mobility ratio, different fracture spacing, different capillary pressure, different relative permeabilities, and varying permeability profiles along the core.

The results of these studies have been upscaled to the field dimensions. The validity of the new definition of characteristic length used in the modified scaling group has been evaluated. The new scaling group used to correlate simulation results has been compared to the early upscaling techniques.

The following conclusions have been derived from this study:

- The comparative study of time rates of water spontaneous imbibition for different types of boundary conditions revealed the fact that the time required for capillary imbibition until residual oil saturation increases exponentially, as the number of faces available for imbibition decreases.

- The comparison of all four types of boundary conditions showed that oil recovery for the All Faces Open type of a model is most efficient and fast, as compared with all other cases.

- The effect of varying permeability profiles along the core on oil recovery showed that when water imbibes in the direction of decreasing permeability, oil recovery is higher than when water imbibes in the direction of increasing permeability.

- The study of the effect of different water-oil viscosity ratios, at which water imbibed into the core, showed that the lower the oil viscosity, the greater the volumes of oil produced from the core as a function of time.

- The results showed that increasing the capillary pressure increased imbibition recovery. Oil recovery by imbibition was sensitive to oil relative permeability curves, while no significant effect was observed in changing the water relative permeability curves.

- A comparative study of time rates of spontaneous imbibition of water for different fracture spacing showed that the time required for capillary imbibition until residual oil saturation increased linearly, as the fracture space increased.

- The characteristic length described by Ma and co-workers37 in the equation of dimensionless time improved a correlation between data points for the models with different boundary conditions.

- The new technique used for upscaling, significantly improved correlations by taking end-point fluid phase mobilities and the mobility ratios into account.

NOMENCLATURE

$A =$ Total area, ft^2

$B_o =$ Bond Number

$D =$ Diameter, ft

$g =$ Gravitational acceleration, ft/sec^2

$H =$ Height, ft

$J(S_w) =$ Leverett J-function

$k =$ Permeability, md

$k_{ro} =$ Oil relative permeability

$k_{rw} =$ Water relative permeability

$L =$ Length, ft

$L_c =$ Characteristic length, ft

$M =$ Mobility ratio

$P_c =$ Capillary pressure, psi

$P_{nw} =$ Pressure of non-wetting phase, psi

$P_w =$ Pressure of wetting phase, psi

$r =$ Pore radius, ft

$R =$ Oil recovery, %

$R_\infty =$ Ultimate recovery, %

$R_{imb} =$ Imbibition oil recovery, %

$S_w =$ Water saturation, fraction

$S_{wi} =$ Irreducible water saturation, fraction

$S_{nwr} =$ Residual saturation, fraction

$S_e =$ Effective water saturation, fraction

$t =$ Time, min

$t_d =$ Dimensionless time

$t_c =$ Dimensionless time for high capillary gravity ratio

$t_g =$ Dimensionless time for low capillary gravity ratio

$V =$ Volume, ft^3

$\mu_o =$ Oil viscosity, cp

$\mu_w =$ Water viscosity, cp

$\mu_g =$ Geometric mean of the water and oil phase viscosities, cp

$\rho =$ Density, ft/lb^3

$\phi =$ Porosity, fraction

$\sigma =$ Interfacial tension, dynes/cm

$\theta =$ Contact angle, degrees

$\lambda =$ Phase mobility, md/cp

REFERENCES

1. Fidra, Y.: "A Study of Imbibition Mechanisms in the Naturally Fractured Spraberry Trend Area," MS thesis, New Mexico Institute of Mining and Technology, Los Lunas, New Mexico (1998).

2. Nelson, R.A.: *Geological Analysis of Naturally Fractured Reservoirs,* second edition, Gulf Professional Publishing, St. Louis (2001).

3. Jaeger, J.S. and Cook, N.G.W.: *Fundamentals of Rock Mechanics*, third edition, Chapman and Hall Ltd., New York City (1979).

4. Aguilera, R.: *Naturally Fractured Reservoirs*, second edition, PennWell Pub. Co., Tulsa (1995).

5. Reiss, L.H.: *The Reservoir Engineering Aspects of Fractured Reservoirs*, Golf. Pub. Co., Houston (1980).

6. Van Golf-Racht, T.D.: *Fundamentals of Fractured Reservoir Engineering*, Elsevier Scientific Pub. Co., Amsterdam (1982).

7. Nelson, R.A.: *Geologic Analysis of Naturally Fractured Reservoirs*, Golf. Pub. Co., Houston (1985).

8. *Rock Fractures and Fluid Flow: Contemporary Understanding and Applications*, Committee on Fracture Characterization and Fluid Flow, National Academy Press, Washington, D.C. (1996).

9. Warren, J.E. and Root, P.J.: "The Behavior of Naturally Fractured Reservoirs," *SPEJ* (September 1963) **245-255**.

10. Brownscombe, E.R., and Dyes, A.B.: "Water-Imbibition Displacement… Can it Release Reluctant Spraberry Oil?," *Oil and Gas J.* (17 November 1952) **264-265**.

11. Kleppe, J., and Morse, R.A.: "Oil Production from Fractured Reservoirs by Water Displacement," paper SPE 5084 presented at the SPE-AIME 49th Annual Fall Meeting, Houston, Texas, 6-9 October.

12. Scheidegger, A.E.: *The Physics of Flow Through Porous Media,* The Macmillan Co., New York, (1960).

13. Dullien, F.A.L.: *Porous Media: Fluid Transport and Pore Structure,* Academic Press, New York (1979).

14. Cox, J.C.: "Surfactant Based Imbibition and Induced Solution Gas Drive Process: Investigation by Nuclear Magnetic Resonance," MS Thesis, Texas A&M University, College Station, Texas, (1993).

15. Brooks, R.H. and Corey, A.T.: "Hydraulic Properties of Porous Media," Hydrology Papers No. 3, Colorado State University, Fort Collins, Colorado, March 1964.

16. Leverett, M.C.: "Flow of Oil-Water Mixtures through Unconsolidated Sands," *Trans.,* AIME, 132, 149 (1939).

17. Barenblatt, G.I., Zheltov, I.P. and Kochina, I.N.: "Basic Concepts in the Theory of Seepage of Homogenous Liquids in Fissured Rocks (Strata)," *J. Appl. Math. Mech.* (1960) 24, **1286-1303.**

18. Chen, J., Miller, M.A., and Sepehrnoori, K.: "Theoretical Investigation of Countercurrent Imbibition in Fractured Reservoir Matrix Blocks," paper SPE 29141 presented at 1995 SPE Symposium on Reservoir Simulation, San Antonio, Texas, 12-15 February.

19. Aronofsky, J.S., Masse, L., and Natanson, S. G.: "A Model for the Mechanism of Oil Recovery from the Porous Matrix Due to Water Invasion in Fractured Reservoirs," *Trans.*, AIME (1958) **213**, 17-19.

20. Handy, L.L.: "Determination of Effective Capillary Pressures for Porous Media from Imbibition Data," *Trans.,* AIME (April 1960) **80**.

21. Iffly, R., Rousselet, D.C., and Vermeulen, J. L.: "Fundamental Study of Imbibition in Fissured Oil Fields," paper SPE 4102 presented at the 1972 SPE Annual Meeting, San-Antonio, Texas, 8-11 October.

22. Civan, F.: "Waterflooding of Naturally Fractured Reservoirs: An Efficient Simulation Approach," paper SPE 25449 presented at the 1993 Production Operations Symposium, Oklahoma City, Oklahoma, 21-23 March.

23. Gupta, A., and Civan, F.: "An Improved Model for Laboratory Measurement of Matrix to Fracture Transfer Function Parameters in Immiscible Displacement," paper SPE 28929 presented at the 1994 SPE Annual Technical Conference and Exhibition, New Orleans, Louisiana, 25-28 September.

24. Civan, F.: "Quadrature Solution for Waterflooding of Naturally Fractured Reservoirs," *SPEREE* (April 1998) **141-147.**

25. Civan, F., Wang, W., and Gupta, A.: "Effect of Wettability and Matrix to Fracture Transfer on the Waterflooding in Fractured Reservoirs," paper SPE 52197 presented at the 1999 SPE Mid-Continent Operations Symposium, Oklahoma City, Oklahoma, 28-31 March.

26. Cil, M., Reis, J.C., Miller M.A., and Misra, D.: "An Examination of Countercurrent Capillary Imbibition Recovery from Single Matrix Blocks and Recovery Predictions by Analytical Matrix/Fracture Transfer Functions," paper SPE 49005 presented at the 1998 SPE Annual Technical Conference, New Orleans, Louisiana, 27-30 September.

27. Rapoport, L.A.: "Scaling Laws for Use in Design and Operation of Water/Oil Flow Models," *Trans*., AIME (1955) **204,** 143.

28. Graham, J.W., and Richardson, J.G.: "Theory and Application of Imbibition Phenomena in Recovery of Oil," *Trans.*, AIME (1959) 216, Technical Note 2029.

29. Mattax, C.C., and Kyte, J.R.: "Imbibition Oil Recovery from Fractured, Water-Drive Reservoirs," *SPEJ* (June 1962) 177-184; *Trans.*, AIME, **225**.

30. Blair, P.M.: "Calculation of Oil Displacement by Countercurrent Water Imbibition," *SPEJ* (September 1964) **195-202.**

31. Du Prey, E.L.: "Gravity and Capillary Effects on Imbibition in Porous Media," *Soc. Pet. Eng. J.* (June, 1978) **195-206.**

32. Hamon, G., and Vidal, J.: "Scaling-Up the Capillary Imbibition Process from Laboratory Experiments on Homogeneous and Heterogeneous Samples," paper SPE 15852 presented at the 1986 SPE European Petroleum Conference, London, 20-22 October.

33. Bourblaux, J., and Kalaidjian, F.J.: "Experimental Study of Co-current and Countercurrent Flows in Naturally Porous Media," paper SPE 18283 presented at the 1988 SPE Annual Technical Conference and Exhibition, Houston, 2-5 October.

34. Kazemi, H., Gilman, J.R., and Elsharkawy, A.M.: "Analytical and Numerical Solution of Oil Recovery from Fractured Reservoirs with Empirical Transfer Functions," paper SPE 6192 presented at the 1976 SPE Annual Technical Conference and Exhibition, New-Orleans, Louisiana, 3-6 October.

35. Akin, S., Kovsek, A.R., and Schembre, J.M.: "Spontaneous Water Imbibition into Diatomite," paper SPE 46211 presented at the 1998 Western Regional Meeting, Bakersfield, California, 10-13 May.

36. Akin, S., and Kovsek, A.R.: "Imbibition Studies of Low-Permeability Porous Media," paper SPE 54590 presented at the 1999 Western Regional Meeting, Anchorage, Alaska, 26-27 May.

37. Ma, S., Zhang, X., and Morrow, N.R.: "Experimental Verification of a Modified Scaling Group for Spontaneous Imbibition," paper SPE 30762 presented at the 1995 SPE Annual Technical Conference and Exhibition, Dallas, Texas, 22-25 October.

38. Cuiec, L., Bourblaux, J., and Kalaidjian, F.: "Oil Recovery by Imbibition in Low-Permeability Chalk," paper SPE 20259 presented at the 1990 SPE/DOE Symposium on Enhanced Oil Recovery, Tulsa, Oklahoma, 22-25 April.

39. Abbasov, M.T., Abbasov, V.A., and Mamedov, R.A.: *Capillary Phenomenon and Oil Recovery*, Elm Publishing House, Baku, Azerbaijan (1987).

40. Kerimova, F.G.: "Studies of Effects of pH of Water on Oil Recovery during the Imbibition," Works of Institute of Deep Oilfield Problems, Baku, Azerbaijan (1990).

41. Guo, B., Schechter D.S., and Baker, R.O.: "An Integrated Study of Imbibition Waterflooding Trend Area Reservoirs in the Naturally Fractured Spraberry," SPE Permian Basin Oil and Gas Recovery Conference, Midland, Texas, 25-27 March 1998.

42. Putra, E., Fidra, Y. and Schechter, D.S.: "Study of Waterflooding Process in Naturally Fractured Reservoirs from Static and Dynamic Imbibition Experiments" Mexico PRRC, Socorro, New Mexico (1998).

43. *Petroleum Engineering Handbook,* H.B. Bradley (ed.), Third Printing, Society of Petroleum Engineers, Richardson, Texas, (1992) **48-9.**

44. Ertekin, T., Abou-Kassem, J.H., and King, G.R.: *Basic Applied Reservoir Simulation*, SPE Textbook Series, SPE, Richardson, Texas (2001) 1, **350-351.**

45. Zhou, D., Jia, L., Kamath, J., and Kovscek, A.R.: "An Investigation of Counter-Current Imbibition Process in Diatomite," paper SPE 68837 presented at the 2001 SPE Western Regional Meeting, Bakersfield, California, 26-30 March.

VITA

Name: Orkhan H. Pashayev

Born: 24 September 1980
                             Baku, Azerbaijan

Permanent Address: 102 Tabriz St, Apt#63
                             Baku, Azerbaijan
                             (opashayev@yahoo.co.uk)

Experience: KBR/Halliburton. July 2001 – July 2002. Title: Process
                             Engineer. Project: ACG Phase 1 – Design of the BP
                             Sangachal Terminal Expansion.

Education: Texas A&M University, College Station, Texas, USA
                             Master of Science Degree in petroleum engineering
                             August 2004

                             Azerbaijan State Oil Academy, Baku, Azerbaijan
                             Bachelor of Science Degree in petroleum engineering
                             July, 2001